People's Democratic Republic of Algeria
الجمـهوريـة الجزائريـة الديمـقراطيـة الشـعبيـة

MINISTRY OF HIGHER EDUCATION AND SCIENTIFIC RESEARCH ——◆—— **HIGHER SCHOOL IN APPLIED SCIENCES --T L E M C E N--**	ESSA Tlemcen-تلمسان المدرسة العليا في العلوم التطبيقية École Supérieure en Sciences Appliquées	وزارة التعليـم العالـي والبحـث العلمـي ———◆——— المـدرسـة العليـا في العلوم التطبيقيـة -تلمسان-

End of study thesis

For obtaining the Engineering degree

Field: **Electrotechnics**
Specialty: **Energy and environment**

Presented by:
Mounir Amine BAKIR
Marwa DOUANE

Theme

Study and simulation of Grid-Side Converter Control for Grid-Connected DFIG Wind Turbines

Publicly defended on 01/ 07/ 2024, before the jury composed of:

Mr M. Mehamedi	MAA	ESSA. Tlemcen	President
Mr A. Chemidi	MCA	ESSA. Tlemcen	Thesis Supervisor
Mr A. Tahour	Professor	ESSA. Tlemcen	Examinator 1
Mr F. Oudjama	MAB	ESSA. Tlemcen	Examinator 2

College year :2023 /2024

بِسْمِ اللَّهِ الرَّحْمَنِ الرَّحِيمِ

Dedication

To **my mother** that I wish more than anything that you were here with me now to make you proud, but continues to be the guiding light that illuminates my path forward.

To **my father** whose selfless sacrifices and tireless efforts have been the driving force behind my academic pursuits.

To **my sister Imen**, standing steadfast through the best of times and the worst. Your unwavering presence has been a true gift. Through every decision, whether joyous or difficult, you have been there to lend an ear, you are not just my sister, but my confidante, my champion, and my saving grace.

To **my only brother hamza** I am forever grateful for the countless ways you have supported me, encouraged me, and believed in me. Your strength has been my strength, the one I can always count on, no matter what.

To **my little sister hanane** I just wanted to take a moment to thank you for being such an amazing sibling. You bring so much joy and love into my life, and I'm so grateful to have you.

To **Feriel Khadidja RAHALI**, my partner in crime, I'm thrilled that our paths crossed, as we've shared countless precious moments and created unforgettable memories over the past few years, from our spontaneous road trips to our late-night conversations about life and everything in between. It was a turning point for me and I will always cherish the lessons I learned from it.

To **Habiba DERKI**, the journey would have been lacking without your unwavering enthusiasm and radiant spirit, which illuminated every step and made our shared experiences truly unforgettable, it' s transformed from ordinary to extraordinary, made our shared experiences a symphony of joy and fulfilment.

To **my constant source of motivation** and support, I am grateful for the enduring bond we share, despite the distance between us. Your continuous commitment to me has been a ray of hope and I am deeply thankful for the unshakeable faith you have on me.

To **my partner Mounir**, this thesis is the fruit of our efforts and our passions and a testimony of our collaboration.

Marwa DOUANE

Dedication

I have the pleasure of dedicating this work to

To my father, this work is dedicated to you, my father who left this world
who allowed me to discover this profession of engineer and who encouraged
me to follow the same path as you.

To my mother, for your support, your affection and your
limitless love, your unwavering trust, your infinite patience
and your immeasurable sacrifices, I humbly dedicate this work to
you.

To my sister, for her encouragement and kindness that she gave
me, I express my deep gratitude and my great respect. This
dedication humbly offered is a testimony of the immeasurable
love I have for you.

To my best friends and to all those who love me and whom I love,

To my partner Marwa who contributed to the completion of this
work.

Mounir Amine BAKIR

Abstract

The main purpose of the work carried out is to analyse a different wind turbine technology integrated into an electrical network, this system behaves a turbine, a generator, rectifier and inventor power converters, these are connected on both sides to the DC bus. The dissertation describes the control and design of a Doubly Fed Induction Generator (DFIG) using back-to-back PWM. This latter is used as the excitation power supply for the DFIG wind power generation, in order to control the stator active and reactive power, a method called direct vector control is based on the transformation of the electrical variables of the machine into a reference that rotates with the flow vector is employed. While the grid side converter is used to regulate the voltage of the DC link capacitor, besides it satisfies the unity power factor of grid-side and bi-direction flowing ability of energy. The control model of whole system is built using MATLAB/Simulink program and the simulation results are discussed by the following.

Keywords: Wind turbines, DFIG, RSC, GSC, vector control, synchronous references, active power, reactive power.

Résumé

Le but principal des travaux réalisés est d'analyser une technologie différente d'éolienne intégrée dans un réseau électrique, ce système comporte une turbine, un générateur, un redresseur et onduleur, des convertisseurs de puissance., ceux-ci sont connectés des deux côtés au bus DC. La thèse décrit le contrôle et la conception d'un générateur asynchrone à double alimentation (MADA) utilisant un convertisseur bidirectionnel PWM. Cette dernière est utilisée comme alimentation d'excitation pour la production d'énergie éolienne avec MADA, afin de contrôler la puissance active et réactive du stator, une méthode appelée la commande vectorielle direct est basée sur la transformation des variables électriques de la machine dans une référence qui tourne avec le vecteur de flux est utilisé. Alors que le convertisseur côté réseau est utilisé pour réguler la tension du condensateur du lien CC, il satisfait en outre un facteur de puissance unitaire côté réseau et une capacité d'écoulement bidirectionnel de l'énergie. Le modèle de contrôle de l'ensemble du système est construit à l'aide du programme MATLAB/Simulink et les résultats de la simulation sont discutés par la suite.

Les mots clés : Les éoliennes, MADA, CCR, CCM, commande vectorielle, références synchrones, puissance active, puissance réactive.

ملخص

الغرض الرئيسي من العمل المنجز هو تحليل تقنية مختلفة لتوربينات الرياح المدمجة في شبكة كهربائية، ويشمل هذا النظام توربينًا ومولدًا ومقومًا وعاكسًا ومحولات طاقة. وهي متصلة على كلا الجانبين بالتيار المستمر. تصف الأطروحة التحكم وتصميم المولد غير المتزامن ذو التغذية المزدوجة باستخدام محول PWM ثنائي الاتجاه لضمان نقل الطاقة بكفاءة بين دوار MADA والشبكة. يتم استخدام الأخير كمصدر طاقة إثارة لإنتاج طاقة الرياح مع MADA بسرعات متغيرة وتردد ثابت، من أجل التحكم في الطاقة النشطة والمتفاعلة للجزء الثابت، تعتمد طريقة تسمى التحكم المباشر في المتجهات على تحويل المتغيرات الكهربائية يتم استخدام الجهاز في مرجع يدور مع ناقل التدفق. في حين يتم استخدام المحول من جانب الشبكة لتنظيم جهد وصلة مكثف التيار المستمر، فإنه يرضي أيضًا عامل طاقة الوحدة من جانب الشبكة وقدرة تدفق الطاقة ثنائية الاتجاه. تم إنشاء نموذج التحكم للنظام بأكمله باستخدام برنامج MATLAB/Simulink وتمت مناقشة نتائج المحاكاة لاحقًا.

Abbreviations

GWEC: Global wind energy council.

HAWT: Horizontal axis wind turbines.

VAWT: Vertical axis wind turbines.

TSR: tip speed ratio.

MPPT: maximum power point tracking.

CLTF: closed loop transfer function.

DFIG: double fed induction generator.

SCIG: squirrel cage induction generator.

WRIG: wound rotor induction generator.

PMSG: permanent magnet synchronous generator.

RSC: rotor side converter.

GSC: grid side converter.

PWM: pulse width modulation.

B2B: back to back.

IGBT: isolated gate bipolar transistor.

FOC: field oriented control.

SFOC: stator flux oriented control.

DFOC: direct field oriented control.

IFOC: indirect field oriented control.

OLTF: opened loop transfer function.

VOC: voltage oriented control.

List of figures

Chapter I

Chapter II

Chapter III

List of Tables

Table of Contents

General introduction

In the last decades, the strong industrialisation, the rising demand for electrical energy and the harmful impacts that fossil fuels bring to the environment and human health, push energy experts to look for new source of energy. In the scenario of alternatives, more and more developing countries are placing their faith in use of renewable energy, it is characterized by its ability to replenish itself naturally, unlike fossil fuels which are finite resources. These pure, limitless energy don't produce greenhouse emissions or air pollutants and reduce the need for environmentally damaging energy extraction processes.

Among the renewable energies, wind energy is considered as an advanced affordable technology and now undergoing rapid development, providing clean electricity for individual home or farm by one wind turbine and for large cities by wind farm alike. Wind energy is old, the first wind turbines (or windmills, as they were originally called) were made from readily available materials, such as wood, formed to blades to pump water for farms, grind grain, sailboats and eventually, power entire communities. Today wind turbines use modern materials to generate clean electrical energy almost anywhere in the world.

Wind turbines, called the windmills of the third millennium, catch the wind energy with propeller-like blades which can have a horizontal axis, like a fan, or vertical, like a merry-go-round, the wind makes the blades spins that powers the generator produces electricity.

Since the early time of developing wind turbines, considerable efforts have been made to utilize three-phase synchronous machines, but for some economic raisons, modern wind power systems use induction machines extensively in wind turbine application. These induction generators fall into two types: fixed speed induction generators (FSIGs) and doubly-fed induction generators (DFIGs). Many of installed wind turbines are equipped with DFIG, which allows a production of electricity for variable-speed, thus allowing better exploitation of wind resources with different wind conditions.

The doubly-fed induction generator has a very important role in the field of electric power generation in wind farms. This type of machine can operate in motor mode as it can operate in generator mode without requiring specific constraints on the value of the speed. This advantage allows the DFIG to operate for a large speed range unlike the synchronous generator that requires a well determined synchronism speed.

This thesis aims to study of electrical energy quality produced by the aerodynamic system and the control of active and reactive powers in our system. Therefore, we will introduce the wind turbine conversion system using a double fed induction generator. The selection of configuration of the converter, control and simulation are described in this work. Within this context, our thesis is structured as follows:

The first chapter will present an overview of wind turbines, followed by its history, main components that describe the system, advantages and drawbacks of the wind energy and the different types of wind turbines, then introduce a theorical notion on the horizontal-axis type. At the end of this part an algorithm called MPPT (maximum power point tracking) is developed whose objective is to maximize the power collected by the wind turbine.

In the second chapter, we will address the different types of generators that used in the wind turbine systems, then find out the best generator based on its advantages compared to others, then we present the modelling of a double fed induction machine in the three-phase reference and in the two-phase reference by adopting the Park transformation, combined with an indirect converter.

The third chapter includes the principle of field-oriented control strategy to control active and reactive stator powers machine side, we will discuss three methods: direct vector control and indirect vector control with and without power loop.

The last chapter contains the control of the grid side converter allows us to regulate the voltage between the terminals of the DC link and also to control the power factor in the connection point with the electrical network. Simulation results are provided at the end of this chapte

Chapter I

Wind turbines; An overview

I.1 Introduction

Wind power is an energy source that has been exploited by mankind for centuries and has since enjoyed the privilege of being the world's leading electricity generator. Long practiced as an engineering form (wind was used to propel ships or to propel waterwheels for hundreds of years), wind power started being taken seriously as an energy source after the oil crisis of the 1970s. At the start of the twenty-first century, and for a fraction of the total transformed energy, it is today one of the most efficient modes of energy production. The ability to generate electricity from wind is mainly due to the development of high-speed turbines. These turbines have improved in efficiency, and have allowed the construction of thousands of wind farms in the last decade. This chapter will present these developments, along with the various wind potentials in the world, the operation of today's wind turbines and the latest advances in wind sensing. We will focus on the conversion of mechanical energy into electricity, offering an interesting overview of the challenges and opportunities that are today driving the wind power industry.

I.2 Description of wind energy

Wind energy is the energy obtained by the force of wind, also called wind kinetic energy, and is used to produce electricity. It is renewable energy, since wind is a renewable, clean and environmentally friendly. This does not mean that it is completely harmless or that it does not cause any negative impact, because everything can have an impact, but this renewable energy has a very low environmental impact compared to non-renewable or other renewables, not to mention that it turns out to be very efficient [1].

I.2.1 Wind turbines

A wind turbine is a machine that converts the kinetic energy of wind into mechanical energy, which is then converted into electricity. It typically consists of a tall tower with large blades mounted on a rotor. When the wind blows, it uses blades to collect the kinetic energy of wind. The wind flows over the blades creating lift (identical to airplane wings), which makes the blades turn. The blades are connected to a drive shaft that turns an electric generator, which produces electricity [2].

I.2.2 History of Wind Turbines

For the first time in known history, a wind-driven wheel is used to power a machine. A Greek engineer, Heron of Alexandria, creates this windwheel.

By 7th to 9th century: Windwheels are used for practical purposes in the Sistan region of Iran, near Afghanistan. The Panemone windmills are used to grind corn, grind flour, and pump water.

By 1000: Windmills are used for pumping seawater to make salt in China and Sicily.

1180s: Vertical windmills are used in Northwestern Europe for grinding flour.

1887: Prof James Blyth built the first known wind turbine in Scotland, installed in his holiday cottage at Marykirk, Scotland. The 10m high turbine charged accumulators developed by Frenchman Camille Alphonse Faure, making it the first house to use wind power.

1888: The first known US wind turbine created for electricity production is built by inventor Charles Brush to provide electricity for his mansion in Ohio (figure I.1).
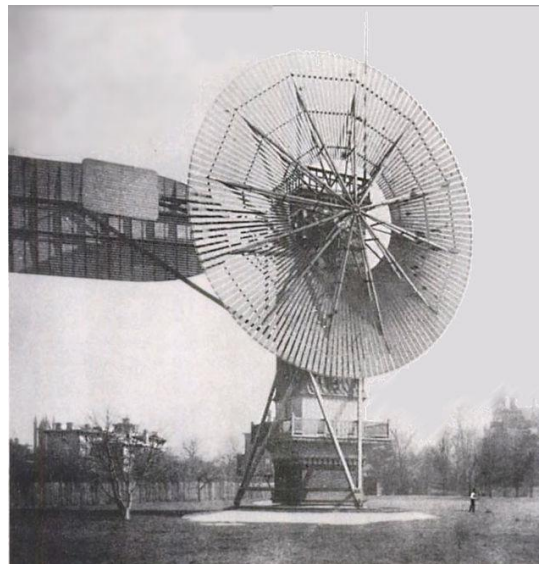
Figure I.1: first known US wind turbine [3]

1903: Poul la Cour starts the Society of Wind Electricians. He is also the first known person to discover that wind turbines with fewer blades that spin faster are more efficient than turbines with many blades spinning slowly.

1931: A horizontal-axis wind turbine similar to the ones we use today is built in Yalta. The wind turbine has 100 kW of capacity, a 32-meter-high tower, and a 32% load.

1975: The first US wind farm is put online, producing enough power for up to 4,149 homes.

1978: The world's first multi-megawatt wind turbine is produced by Tvind school teachers and students. The 2-megawatt wind turbine pioneered many technologies used in modern wind turbines.

1995: Production of first offshore wind turbine.

By the 19th century, the average number of wind turbines around the world was increasing, and the power capacity was thousands of megawatts. Governments began investing in wind energy research and development, leading to significant technological advancements. In 2013 wind power produces more electricity than any other source in Spain for three months in a row [3].

I.2.3 Main components of a wind turbine

The vocabulary most often used to describe a wind turbine mainly includes four sub-system:

The nacelle: is a large, box-shaped structure that houses the turbine's generator, gearbox and other key components. It is typically mounted on top of the wind turbine tower and is designed to protect the sensitive components from harsh outdoor elements. The nacelle also contains various sensors and control systems that monitor the performance of the turbine and adjust its operation accordingly [4].

Towers: are the structural base of the wind turbine that support the rotor and the nacelle module. There are three main types of towers used in large wind turbines: tubular steel towers, lattice towers, and hybrid towers [5].
The tower, consisting of the mast, the electrical control system and the transformer. Usually conical in shape, the mast can withstand the navel. Its height varies between 50 and 130 m high and has a foot diameter between 4 and 7 m. An opening at the bottom of the mast allows access to the various equipment of the wind turbine, among which the transformer that allows to increase the voltage of the electricity produced in order to inject it into the grid [6].

The foundation: it is a large, heavy structural block of concrete in the ground that supports the entire turbine and the forces acting on it. In offshore turbines, the foundation is underwater [7].

The rotor and hub: A turbine rotor is at the heart of a turbine – with mounted blades on this rotating part. Turbine rotors convert energy from their surroundings (Wind), into kinetic energy, by moving at their high speed. This kinetic energy is then converted into mechanical work and transformed via a gearbox into electrical power. It consists of three blades and a central part connecting the blades, the hub, its function is to hold the blades and allow them to rotate relative to the rest of the turbine body [8].

Although it is the most common, a turbine does not necessarily have three blades. But the three-blade rotor has advantages such as optimum efficiency. For aerodynamics, the blades are

shaped like an air foil (like an airplane's wings). Also, they are not flat and have a twist between their root and tip. The blade can rotate up to 90° around its axis. This movement is called pitch [9].
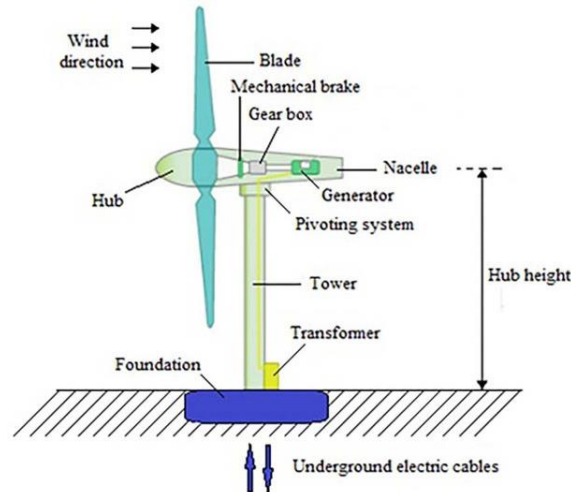
Figure I.2: Main components of a wind turbine [10]

I.2.4 Advantages and drawbacks of wind energy

Advantages

-Wind energy is a clean, renewable energy source that produces neither pollution nor wastes. Moreover, it can repay its energy debt, in a few months, because wind turbines do not need much maintenance to keep them running, compared to coal and nuclear power plants.

-Wind power is known for its exceptional energy efficiency. According to the U.S. Energy Information Administration, the average wind turbine in the United States generates over 843,000 kilowatt-hours per month, enough to power 940 homes.

-Unlike other power plants that need lots of space and cannot be around agriculture and industry, wind turbine can be built in areas with high and consistent wind speeds such as mountain passes and ridges, offshore locations, seas, deserts, airports, highways and major roads, coastal areas.

-As the wind sector grows, the demand for workers who can develop, operate, construct, and maintain wind projects will inevitably grow too. In 2021, the Global Wind Energy Council (GWEC) reported that 3.3 million new wind power jobs could be generated globally over the next five years [11].

Drawbacks

-Visual and sound pollution. Interference from electromagnetic waves (TV, radio, mobile phones) constitutes an obstacle to private residential facilities, which requires installing wind turbines away from the residence.

- Although the cost of wind power has been decreasing as it has grown in use, the start-up cost is still very high. Multiple wind turbines can also get quite expensive, the average wind turbine costs around $1,200,000 per megawatt of electricity-generating capacity.

- Biologically, wind turbines are responsible for many bird and bat deaths worldwide. Spinning turbine blades kill over a million birds annually in the United States alone. In the case of bats, they die from an effect called barotrauma, it happens when bats fly too close to a wind turbine. The sudden pressure drop-in air caused by the movement of the turbine's blades can damage a bat's lungs, causing it to die.

Wind turbines cause noise and visual pollution, in rural areas with few inhabitants which host most wind turbine farms. The noises from the construction phase of a wind project, heavy equipment and transport trucks can also disturb the local community [12].

I.2.5 Different types of wind turbines

I.2.5.1 Horizontal Axis Wind Turbines (HAWT)

Horizontal axis wind turbines usually have three blades, like airplane propellers. They're placed on a tall tower, with all their parts, including the blades, shaft, and generator, on top. The blades point towards the wind, and the shaft is flat. Most of the wind turbines we see are horizontal wind turbine. HAWTs are suitable for both small-scale residential installations and large utility-scale wind farms. They can generate electricity with capacities ranging from 1 kW to over 10 MW [13].

I.2.5.2 Vertical Axis Wind Turbines (VAWT)

The vertical-axis wind turbines have blades that are attached to the top and the bottom of a vertical rotor. They can capture wind from any direction and are often used in urban environments or where aesthetics is a concern. One of the main advantages of this type of wind

turbine is that it succeeds in capturing weak winds and producing energy even with a lighter wind speed [13].

Among the vertical wind turbines, two types stand out today on the market:

Savonius Rotors: developed by Finnish engineer Savonius, it distinguished by its relatively large and drag-driven design. The shape is made up of two semi-cylinders that are rotated 90 degrees with respect to each other and positioned on the outside of the axis. This type of vertical wind turbine has many advantages including the fact that it can be installed in places with high wind speed and make very little noise compared to other Wind turbines on the market. The disadvantage of this type of wind turbine is that it needs a relatively strong wind to start turning and thus to produce energy.

Darrieus Rotors: developed by a French engineer Darrieus, it's a lift-type vertical axis wind turbine, means that it uses the aerodynamic force of lift to spin the blades. The rotation of the wind turbine is produced by the lift created by a series of lift blades with air foil-like cross sections. Darrieus rotors have higher efficiency compared to Savonius rotors [14].

And other two types of vertical wind turbines:

H-Rotors: type of the Darrieus rotor, unlike the traditional model, the turbine's blades are straight instead of curved. Theoretically producing more power than models with curved blades because the H-rotor's larger surface area works against the wind.

Helical Rotors: They have spiral or helix-shaped curving blades around a vertical shaft. The rotor can catch wind from many directions because to its spiral shape, which eliminates the need for complex mechanisms to rotate and face the wind [15].
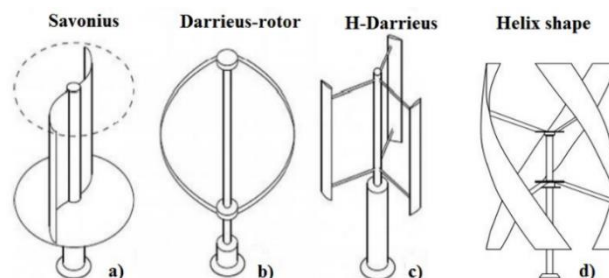
Figure I.3: The most common types of wind turbines [16]

I.2.5.3 Vortex: The World's First Bladeless Turbine

The Vortex Bladeless wind turbine, it uses a phenomenon called "vortex shedding" to generate power electricity. Vortex Bladeless vibrates on low to medium wind speeds using the power contained in its vortices that is generated when wind bypasses the structure and transforms mechanical energy into electricity.

They made to deal with problems of conventional wind turbines, such noise, operating costs, and their impact on birds. Three different versions of the Vortex Bladeless are now under development, two of those prototypes are in service. Vortex Nano is the small model with 1m height and a power output of 3 W, vortex Tacoma is standing at a height of 2.75 m with a power output of 100 W and Vortex Atlantis (Grand), it is a prototype for the moment with 9 to 13 m tall and has a power output of approximately 1 kW [17].
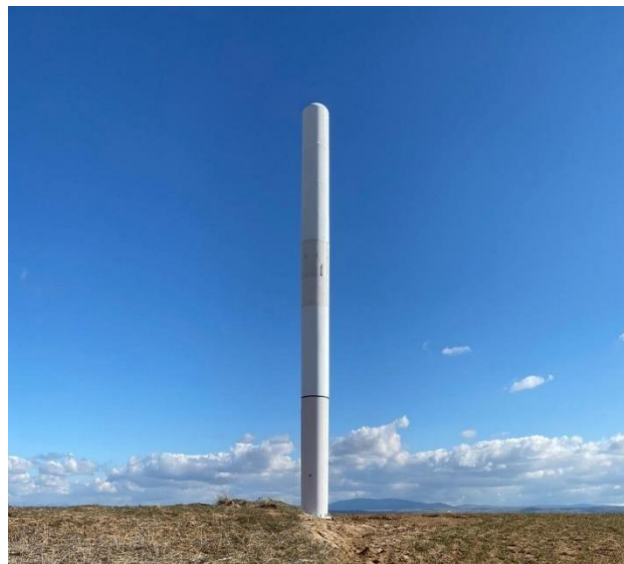
Figure I.4: Vortex Wind turbine [18]

I.3 The Wind

I.3.1 Definition of wind

The definition of "wind" refers to the natural movement of air in the Earth's atmosphere, typically caused by the uneven heating of the Earth's surface by the sun. It is characterized by its direction, speed, and force, wind is the primary source of energy that drives the rotation of the turbine blades.

Air masses can migrate from one region to another as a result of differences in air pressure. From high air pressure regions to low air pressure regions, air masses often move. As a result, winds blow toward low-pressure zones and away from high-pressure areas.

I.3.2 Wind measurements

I.3.2.1 Wind speed

At a given point and at a specific time, air moves horizontally in a specific direction. Its speed, called "wind speed", is then determined. This speed is usually expressed in meters per second (m/s), kilometres per hour (km/h), or in knots or miles per hour. To measure this speed, the most commonly used tool is the cup anemometer. This device is equipped with a rotor consisting of three cups which, under the effect of wind, rotate around a vertical axis. The rotation of these cups is then recorded electronically, the data collected by anemometers is useful for various applications, including weather forecasting, wind energy projects, and safety assessments in outdoor environments.

I.3.2.2 Wind direction

The wind direction is indicated by a weather vane, often known as a wind vane. A wind vane determines the direction of the wind, it points toward the source of the wind.
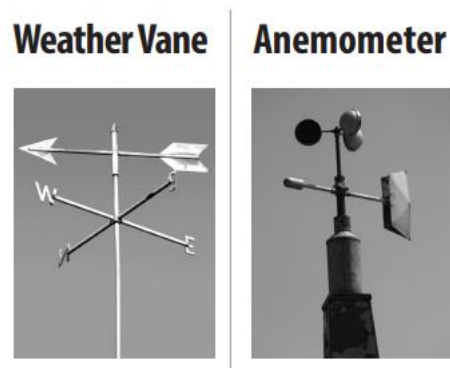
Figure I.5: speed and direction measurement devices [19]

I.3.2.3 Wind measurement pylons

Generally speaking, wind data that is accessible for all nations was gathered close to towns. People assemble in places sheltered from strong winds and storms. As a result, information from meteorological stations, military sites, and airports is not necessarily indicative of the wind that blows in exposed regions, and the wind potential of certain places may be overestimated.

In order to monitor wind characteristics, masters must be planted in appropriate locations. They commonly known as anemometer towers or meteorological towers; they are made with maximum permeability to the wind to reduce interference with the measurements. Usually, the pylons consist of triangular-shaped tubular steel trusses. To sustain the pylon construction, they employ three sets of pre-stressed cables positioned at various heights.

Figure I.6: Wind measurement pylons [20]

According to ISO 61400-12-1 [21], the measuring devices (wind vanes, anemometers, etc.) are mounted on boom arms at a predetermined height and distance from the pylon surface.

I.4 Theoretical notions on the horizontal-axis wind turbine

Not all the available wind energy can be transformed into usable electrical power. During the conversion of kinetic energy due to wind into mechanical energy in the shaft, the available wind potential experiences a series of losses until the electrical energy comes out of the generator. At the end of the process, only part of the wind power available at specific location is actually collected.
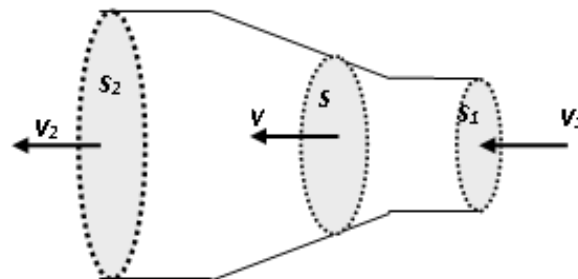
Figure I.7: Air current tube around a wind turbine [22]

The formula of available power in the wind P_v passing through the swept area S formed by the rotor blades of the wind turbine is given by [23]:

$$P_v = \frac{1}{2}\rho S V^3 \qquad\qquad (I.1)$$

Where P_v is the power in watts, ρ is the density of the air equal 1,225 kg/m³ at sea level, S the swept area of blades in m² and V is velocity of the wind.

The swept area S has the same formula of the area of a circle as shown in equation I.2

$$S = \pi.R^2 \qquad\qquad (I.2)$$

Where *r* is the radius of the circle equals to the length of one rotor blade.

I.4.1 The power coefficient

The power coefficient (Cp) is defined as the ratio of the power extracted by the wind turbine relative to the energy available in the wind stream. The power coefficient Cp is a non-linear function that depends on factors like the tip speed ratio (λ) and pitch angle (θ) of the turbine blades, as written in the following equation [24].

$$Cp = \frac{\text{Electricity produced by wind turbine}}{\text{Total Energy available in the wind}} = \frac{P_t}{P} = \frac{P_t}{\frac{1}{2}\rho\pi R^2 V^3} \qquad\qquad (I.3)$$

I.4.2 The Betz limit

German scientist Albert Betz determined that no wind turbine could transform more than 59.3% of the wind's kinetic energy into mechanical energy that turning a rotor. This is the coefficient of performance, or the percentage of the air energy that can be captured by the wind turbine at its optimum performance and is referred to as the Betz Limit.

$$C_p = \frac{16}{27} = 0{,}593 \qquad\qquad (I.4)$$

In the picture shown below, the wind turbine converts 70% of the Betz Limit into electricity. Therefore, the Cp of this wind turbine would be 0.7 x 0.59 = 0.41. So, this wind turbine converts 41% of the available wind energy into electricity. This is actually a pretty good coefficient of power. Good wind turbines generally fall in the 35-45% range [25].
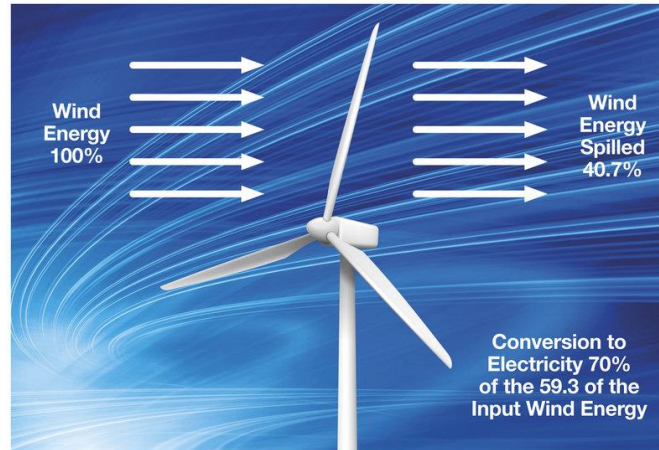
Figure I.8: Wind energy and wind energy spilled [26]

I.4.3 The Tip Speed Ratio (TSR)

It is the ratio between the speed of the blade tips and the speed of the wind. This parameter, also known as the "specific speed" (λ), it indicates how the rotational speed of the turbine blades compares to the wind speed, used to classify wind turbines based on their speed characteristics.

$$\lambda = \frac{\Omega.R}{V}$$ (I.5)

λ: specific speed.

R: length of the pales or radius of the turbine in m.

V: Wind speed in m/s.

Ω: tangential velocity at rotor tip (rad/s) [27].

If the TSR (λ) is less than 3, the wind turbine is considered a "slow" turbine.

If the TSR (λ) is greater than 3, the wind turbine is considered a "fast" turbine.

I.4.4 Classification of wind turbines by power coefficient

The graph below shows at first that air generators with horizontal and vertical axes of the darrieus type have better aerodynamic efficiency. In addition, their power coefficient decreases slowly as the speed increases. American generators have a large number of blades because they move at low rotation speeds, they produce a large aerodynamic torque in order to produce mechanical energy. Triple wind turbines are the most common because they represent a compromise between the vibrations caused by rotation and the cost of the generator. In addition,

their power coefficient reaches high values and decreases slowly as the speed increases. They rarely operate below a wind speed of 3 m/s [22].

Savonius turbine generates high positive torque due to its symmetrical design in any wind direction compared to the Darrieus turbine. It also operates quietly at a lower λ [28]
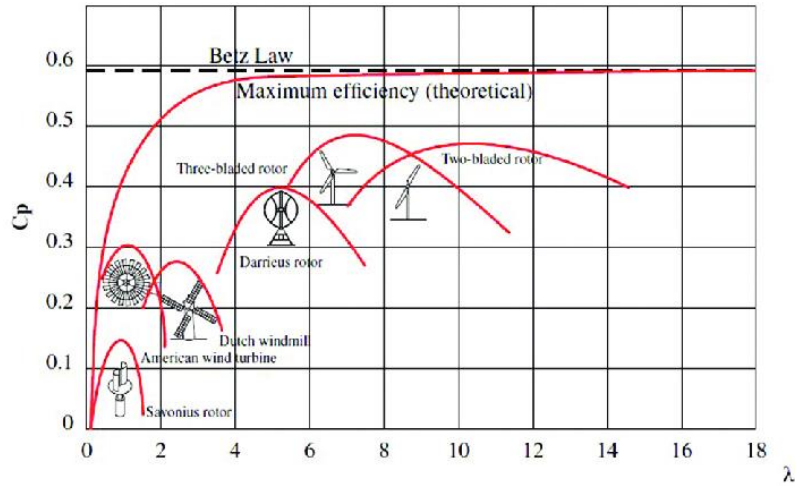
Figure I.9: Tip speed ratio vs power coefficient for various types of Wind turbines [28]

I.4.5 The couple coefficient

The couple coefficient is a crucial parameter that helps in understanding the relationship between the power output efficiency of the turbine and the rotational speed of the blades. It provides insights into how effectively the turbine is converting the available wind energy into mechanical power.

Combining the equations (I.1), (I.6), (I.7) with the mechanical power P_m available on a generator tree which is expressed as follows [22]:

$$P_m = P_{max} = \frac{16}{27}.P_v = 0.59 p_V \tag{I.6}$$

$$C_P^{max} = \frac{P_{max}}{P_v} = \frac{2.P_{max}}{\rho.S.V_v^3} \leq 0.59 \tag{I.7}$$

$$P_m = \frac{P_m}{P_v}.P_v = C_p(\lambda).P_v = \frac{1}{2}C_p(\lambda).\rho\pi R^2.V_v^3 \tag{I.8}$$

Taking into account the ratio of the K speed multiplier, the mechanical power P_m available on the electric generator tree is expressed by:

$$P_m = \frac{1}{2}C_p\left(\frac{R.\Omega}{K.V_v}\right)\rho\pi R^2.V_v^3 \tag{I.9}$$

The aerodynamic torque produced by this wind turbine (theoretical torque) is then deducted:

$$C_T = \frac{P_m}{\Omega} = \frac{1}{2}\left(\frac{C_p(\lambda)}{\Omega}\right)\rho\pi R^2.V_v^3 \tag{I.10}$$

We get $C_c(\lambda) = \frac{C_p(\lambda)}{\lambda}$,the couple coefficient and we get the following relation:

$$C_T = \frac{1}{2}C_c(\lambda)\rho\pi R^3.V_v^2 \tag{I.11}$$

I.5 Maximum Power Point Tracking (MPPT)

A typical wind turbine Power-Speed characteristic is plotted in figure (I.10), there are four functioning areas, depending on the velocity.
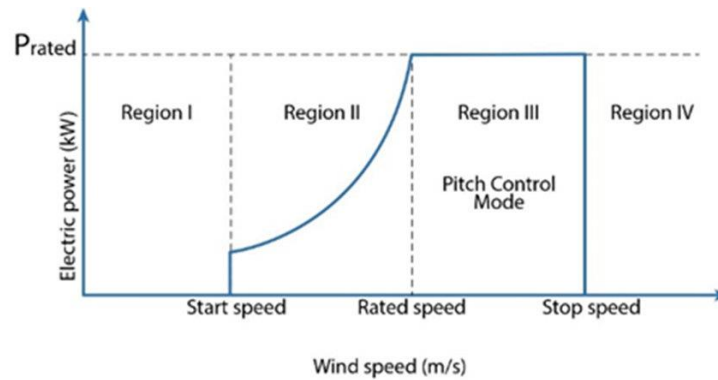
Figure I.10: Operating regions of a Wind turbine [29]

 Regions 1 and 4 are unfeasible, because no reliable power output can be expected before the start speed and after stop speed, hence, the wind turbine operation during this period is not recommended for grid connection. The second region is the optimal zone for power generation via WECS (wind energy conversion system). Moreover, maximum power point operation is possible only when wind turbine has to be operated in this region [30].

As the turbine in the third region has already attained its maximum power, control over the mechanical output power is necessary. Based on the explanation above, region 2 is the best region to employ the maximum power point tracking MPPT.

There are two families of control strategies: MPPT strategy with and without speed control.

I.5.1 MPPT strategy without speed control

The MPPT technique without mechanical speed control consists of the estimation of the quantities that characterize an optimal operating state of wind turbine. Therefore, we assume that the wind speed variation is neglected against the electrical time constants of the wind turbine.

The gearbox converts the slow rotational speed of the turbine to the high mechanical speed required by generator. This multiplier is modelled by a gain G. In principle, the distribution of the total moment of inertia J on the rotating shaft can be written [31]

$$J = \frac{J_t}{G^2} + J_g \tag{I.12}$$

Where J_t and J_g are respectively the moments of inertia on the turbine and on the generator of the machine. Thus, modelling the transmission of mechanical energy can be summarised following the equation (I.12)

$$J = \frac{d\Omega_g}{dt} = C_{mec} = C_g - C_{em} - C_f \tag{I.13}$$

Where:

C_g: Multiplier torque applying to the generator shaft.

C_{em}: Generated electromagnetic torque.

$C_f = f_v \Omega_g$: The torque of viscous friction.

The block diagram of the turbine model with double fed induction generator DFIG is schematized in figure (I.11), which groups the preceding equations together:
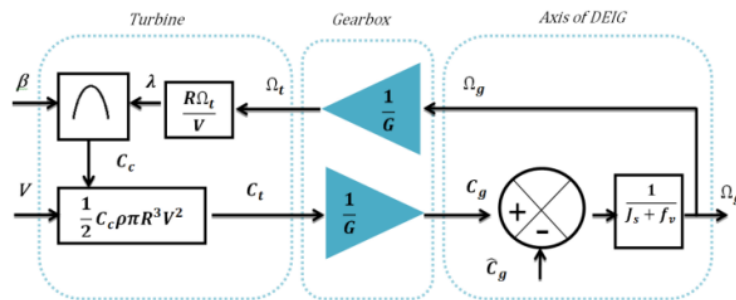
Figure I.11: Block diagram of the model turbine [31]

In order to maximize the amount of wind energy, we must continually adjust the turbine's rotational speed according to the variations of the wind speed [32]. The principle of this command is always to have a turbine rotational speed, allows an optimal speed ratio $\lambda = \lambda_{opt}$. The electromagnetic torque reference is obtained by estimating the wind speed which, in its turn, determined from the measurement of mechanical rotational speed. This magnitude in equation (I.17), deduced from equations (I.14), (I.15), (I.16) [33].

$$\widehat{\Omega_t} = \frac{\Omega_g}{G} \tag{I.14}$$

$$\hat{V} = \frac{\widehat{\Omega}_{aer}.R}{\lambda_{opt}} \tag{I.15}$$

$$\hat{C}_{aer} = \frac{1}{2} C_c^{max} \rho \pi R^3 \tag{I.16}$$

$$\hat{C}_g^* = \frac{\hat{C}_{aer}^*}{G} = \frac{1}{2G\lambda_{opt}^2} C_c^{max} \rho \pi R^5 \hat{\Omega}_t^2 \tag{I.17}$$

The following figure is the control strategy without wind speed measurement
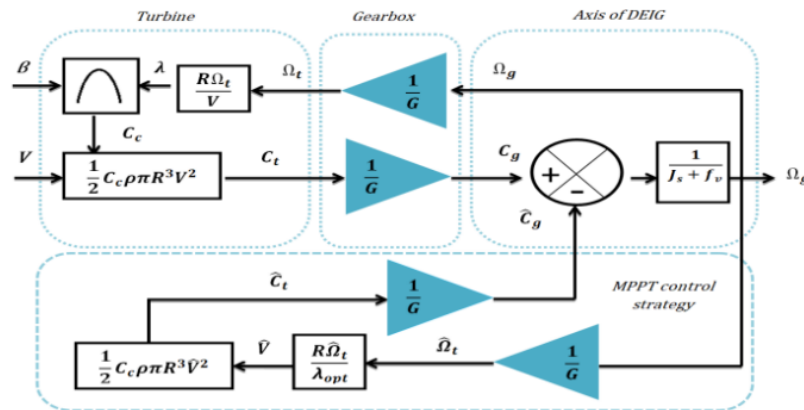
Figure I.12: MPPT strategy without wind speed control

I.5.2 MPPT strategy with speed control

The control algorithms strategy consists of adjusting the generator's electromagnetic torque to push the mechanical speed to pursue a reference value. The latter will maximize the extracted power of the turbine Consequently, the speed of the generator must be controlled. considering the mechanical torque Cg as a disturbance the MPPT controller consists of Equation (I.18) for the estimation of the reference rotational speed of the turbine, Equation (I.19) for calculating

the reference mechanical speed, and the transfer function of the proportional integral (PI) regulator.

$$V_{est} = \frac{\Omega_{turbine}.R}{\lambda_{opt}}$$ (I.18)

$$\Omega_{turbine} = \frac{\Omega_{mec}}{G}$$ (I.19)

All this is associated with the model of figure (I.13) [34].
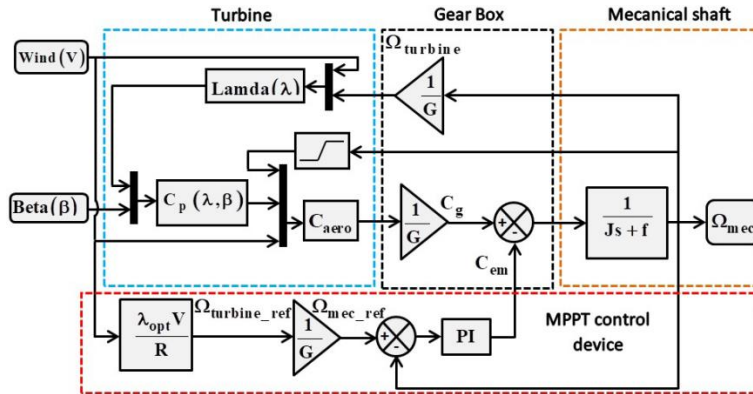
Figure I.13: MPPT with PI control of the mechanical speed of the wind turbine

I.5.2.1 PI regulator for MPPT with speed control

The principle of the regulation synthesis given in Figure (I.13). The latter will allow us to establish a relationship between the function of the corrector C(s) of the PI and the transfer function of the model of the mechanical shaft G(s), in order to determine the values of the coefficients K_P and K_I which will allow the PI corrector to regulate the mechanical speed [34].
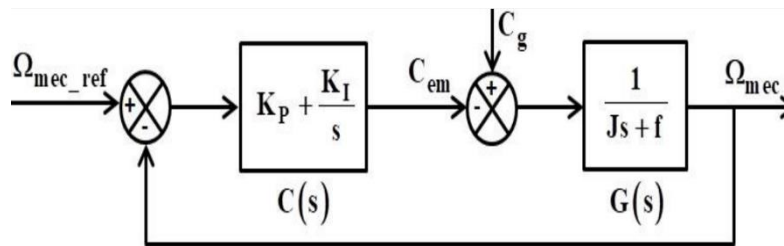
Figure I.14: Principle of MPPT regulation with PI control

The Closed Loop Transfer Function (CLTF) is given by the following Expression

$$CLTF = \frac{C(s).G(s)}{C(s).G(s)+1}$$ (I.20)

According to figure (I.14), by replacing the transfer functions by its equations, we get

$$CLTF = \frac{\left(K_p + \frac{K_I}{s}\right)\left(\frac{1}{j.s+f}\right)}{\left(K_p + \frac{K_I}{s}\right)\left(\frac{1}{j.s+f}\right) + 1}$$

After simplification, we obtain.

$$CLTF = \frac{\left(\frac{K_p}{j}s + \frac{K_I}{j}\right)}{s^2 + \left(\frac{f+Kp}{j}\right)s + \frac{K_I}{j}} \tag{I.21}$$

By identifying the *CLTF* with a transfer function of a 2nd order filter, we deduce the proportional and integral coefficients expressions:

$$\begin{cases} K_I = \omega_0^2.j \\ K_p = 2\xi\omega_0 j - f \end{cases} \tag{I.22}$$

The response time is given by

$$\tau_r(n) = \frac{1}{\xi\omega_0}\left(\frac{100}{n}\right) \tag{I.23}$$

n: Actual value of the depreciation rate; ξ: Damping rate; ω_0: Filter cutoff pulse.

I.6 Conclusion:

This chapter provides a brief introduction to the field of wind energy. It addresses the basic concepts of wind technology, we began by exploring wind energy's definition and highlighting its value as a clean, renewable energy source, then their historical development from its humble beginnings to recent advances in technologies of wind turbine. Next, we examined a wind turbine's essential components, showing their function to generate electricity from wind energy. We touched both benefits and drawbacks of wind energy, emphasizing its environmental benefits and operational challenges. Furthermore, the chapter delves into the different types of wind turbines, throw light on the variety of designs suited to various energy requirements and environmental circumstances. Additionally, it touches wind measurements, underlining the importance of accurate data for efficient turbine operation. Theoretical notions on the horizontal-axis wind turbine are discussed, clarifying the aerodynamics and mechanics behind

their functionality, also covers maximum power point tracking MPPT strategies with and without speed control, which are necessary for maximizing energy extraction.

The next chapter includes a representation and modelling of double fed induction generator DFIG which is commonly used in wind conversion systems.

Chapter II
Double fed induction generator (DFIG) modelling

II.1 Introduction

Wind turbine is a device that converts kinetic energy of the wind into electrical energy. These days, the most use type of wind turbine is the horizontal axis wind turbine. Wind turbines are classified into two categories variable speed or fixed speed. In fixed speed turbines the maximum efficiency is obtained at a particular speed only and device consist of an induction generator connected directly to the grid. To lower reactive power consumption, a soft starting unit plus capacitor bank installation are needed. Fixed speed turbines are easy to operate, reliable, affordable, powerful, and well certified. Also, electrical parts are reasonably priced. The drawbacks are mechanical strain from fixed speed operation, prohibited power quality control, and uncontrolled reactive power consumption.

The greatest efficiency of variable speed wind turbines is achieved throughout a wide range of wind speeds. Compared to fixed speed wind turbines, the electrical system design of variable speed wind turbines is more complex, it has a synchronous or induction generator that is linked to the grid via a power converter which is used to control the speed of the generator, their upsides are reducing mechanical stress, better power quality, and increased energy capture, but the equipment is pricey, and its design is complex.

Nowadays, the most commonly used generator in wind turbines is the wound rotor induction generator, known as a doubly fed induction generator (DFIG). The structure of the chapter is organized as following: first, we will address the different types of generators that used in the wind turbine systems, then find out the best generator based on its advantages compared to others and present the modelling of the wind energy conversion system linked to the generator.

II.2 Types of generators used in Wind Turbine System

Any types of three-phase generator can connect with a wind turbine, some are often used in fixed-speed wind turbines, where the rotor speed is fixed and connected directly to the grid, while other are favoured for variable-speed wind turbines, offering advantages such as increased energy capture and reduced mechanical stress. The following are the different types of generators that are utilized in wind turbines, detailed explanation is given.

II.2.1 Asynchronous Generators

II.2.1.1 Squirrel Cage Induction Generator

It is commonly used in fixed-speed wind turbines systems, the SCIG motor is directly connected to the wind through a transformer, with the rotor speed fixed to the frequency of the grid, making it operate at a constant speed Reactive power compensation is provided by a bank of capacitors, and a soft starter facilitates a smooth grid connection. The main drawback is not supporting any speed control [35].
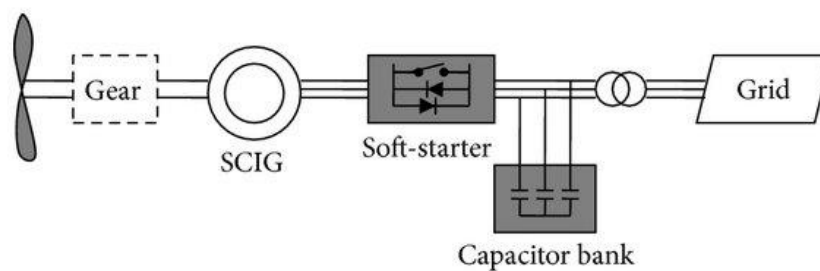
Figure II.1: A wind turbine with a squirrel Cage Induction Generator [35]

II.2.1.2 Wound rotor induction generator (WRIG)

Wound Rotor Induction Generator use the concept of variable speed, it is directly connected to the grid as shown in the figure. It's different from the SCIG because it contains a variable rotor resistance for controlling power output of the generator, a soft starter is used here for reduce inrush current and a compensator to eliminate the reactive power demand. The disadvantages of this configuration are poor control of active, reactive power and a limited speed range.
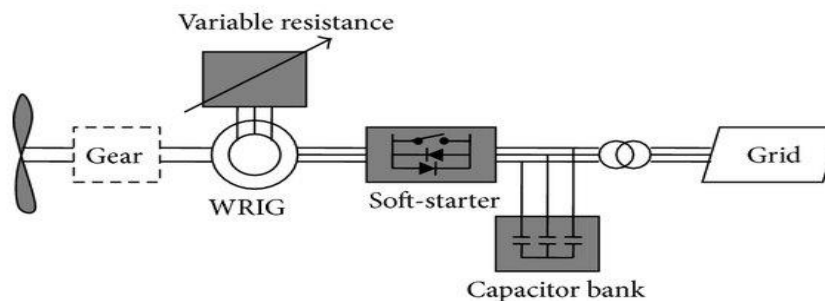
Figure II.2: A wind turbine with a WRI generator [35]

II.2.2 Synchronous Generator

II.2.2.1 Wound Rotor Generator

This configuration doesn't require soft starter and the reactive power comparator is replaced with a partial scale frequency converter which is used for the compensation of reactive power and smoothing grid connection, but in the case of grid fault, it is required for additional protection and using slip rings, the configuration is shown in figure [35].
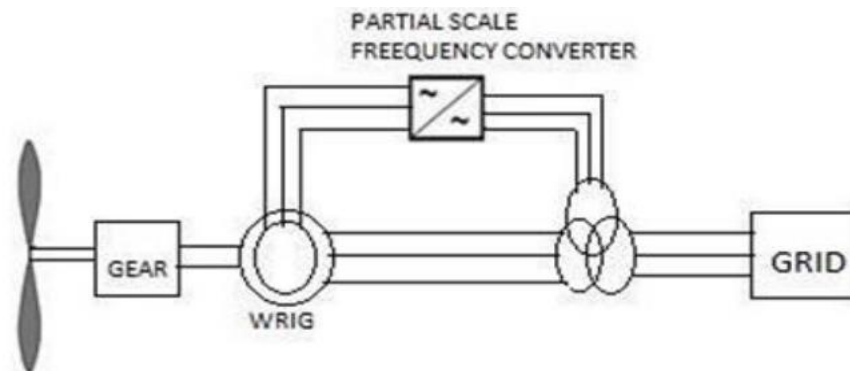
Figure II.3: wound rotor generator configuration

II.2.2.2 Permanent Magnet Generator

A PMSG is a synchronous generator its rotor uses permanent magnets to produce the magnetic field, that's mean its rotor speed is synchronized with the frequency of the grid connected to the grid by full scale frequency converter which helps controlling both the active and reactive power, as gives in figure (II.4) [35].
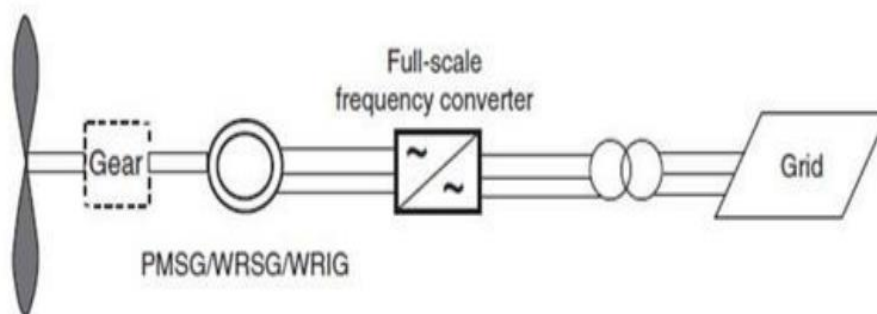
Figure II.4: Permanent magnet synchronous generator

II.2.3 Doubly Fed Induction Generator

The Doubly Fed Induction Generator (DFIG) is a type of generators, that uses a doubly-fed induction to convert the mechanical energy from the wind into electrical energy. The stator part

of the generator is directly connected to the grid while the rotor is interfaced through an AC-DC-AC power converter that controls both the active and reactive power flow and a crowbar which is installed between the generator and converter in order to prevent short circuits in the wind energy system [35].
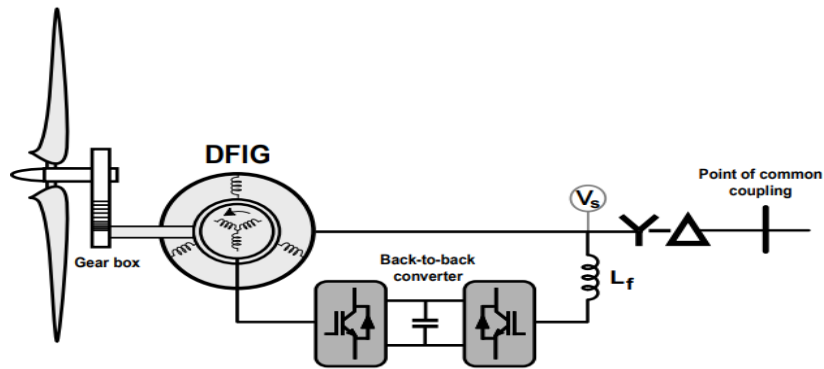
FigureII.5: Doubly fed induction generator wind turbine

II.3 Double fed induction generator modelling

The basic concept scheme of DFIG used in most systems is seen in figure below (II.6). The wound rotor is supplied from the power electronics converter via slip rings, allowing DFIG to run at different speeds in response to variations in wind speed. The stator is directly linked to the grid.
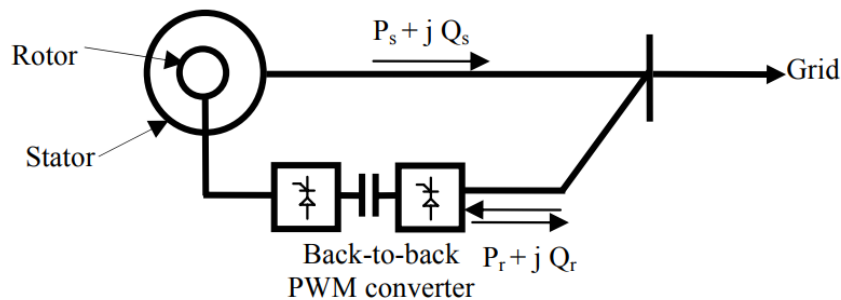
Figure II.6: Simplified schematic diagram of Doubly-Fed Induction Generator

II.3.1 Description of wind turbine based on the DFIG

The general block diagram for controlling a DFIG is shown in Figure (II.6). The basic parts of model consist of the mechanical part which includes the turbine rotor, drive train, and pitch angle controller, Doubly-Fed Induction Generator (DFIG), a back-to-back converter consists of a rotor-side converter (RSC) that controls the DFIG torque and speed and a grid-side converter (GSC) that transfers the rotor power to the grid and maintains the DC-link voltage.

They are connected by a DC-link capacitor, and employ PWM modulation.

B2B converter is bidirectional converter type, modelled with bidirectional switches, therefore, both converters operate as rectifiers or inverters. The difference between them is the definition of the power sign, where the ideal switch is created by a semiconductor with an anti-parallel diode allowing current to flow in both directions. The semiconductor used is an isolated gate bipolar transistor (IGBT) with ideal operation [36].
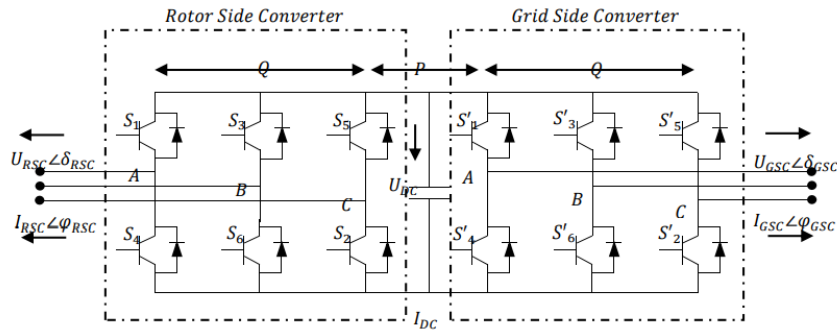
Figure II.7: B2B power converter configuration [36]

In fact, the DFIG allows hypo-synchronous and hyper-synchronous, which refer to the operation of the machine relative to its synchronous speed.

S is the slip, its formula:

$$S = \frac{\omega_S - \omega_r}{\omega_S} = \frac{\Omega_S - \Omega_r}{\Omega_S} \tag{II.1}$$

The slip is the difference between synchronization speed and rotor speed. When the rotational speed of the DFIG is lower than the synchronous speed, it is in the hypo-synchronous mode, in this case, the slip is positive, and the machine operates as a motor. The DFIG functions in the hyper-synchronous mode when its rotating speed is higher than the synchronous speed, in this situation, the machine acts as a generator since the slip is negative [37].

II.3.2 Representation of DFIG in abc-coordinates

The three-phase asynchronous machine consists of a fixed stator and a mobile cylindrical rotor. The stator has three wrappings coupled in a star or triangle and are powered by a three-phase voltage system. This results the creation of a magnetic field slipping into the machine entrance.
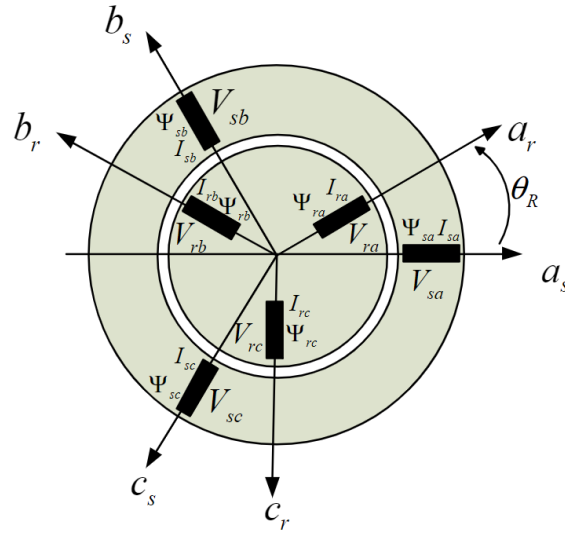
Figure II.8: Spatial representation of the DFIG in the triphasic reference [37]

With: a_S, b_S, c_S are vectors oriented according to stator windings.

a_r, b_r, c_r are vectors oriented according to rotor windings.

θ is the position angle between the stator and the rotor.

The model used is based on the following classical simplifying assumptions [38]:

A sinusoidal spatial distribution of magnetic induction through the air gap is allowed.

Induced currents in the magnetic circuit are neglected (Foucault current).

Magnetic saturation in the DFIG is neglected.

Flux distribution is sinusoidal.

the winding resistances are considered to be constant.

These assumptions reduce the complexity of the modelling task and the amount of system data that is needed.

The voltage equations of the asynchronous machine in a-b-c reference frame are given in matrix form by the following relationships [37]:

$$[V_S] = [R_S].[I_S] + \frac{d}{dt}[\psi_S] \qquad (II.2)$$

$$[V_r] = [R_r].[I_r] + \frac{d}{dt}[\psi_r] \qquad (II.3)$$

We have: $[V_S] = [V_{sa}, V_{sb}, V_{sc}]^T$ and $[V_r] = [V_{ra}, V_{rb}, V_{rc}]^T$ are the voltages of the three phases to the stator and rotor.

$[I_S] = [I_{sa}, I_{sb}, I_{sc}]^T$ and $[i_r] = [I_{ra}, I_{rb}, I_{rc}]^T$ are the currents of the three phases to the stator and rotor.

$[\psi_S] = [\phi_{sa}, \phi_{sb}, \phi_{sc}]^T$ and $[\psi_r] = [\phi_{ra}, \phi_{rb}, \phi_{rc}]^T$ are the vectors of the total flow through the windings of the stator and rotor.

$$[R_S] = \begin{bmatrix} R_s & 0 & 0 \\ 0 & R_s & 0 \\ 0 & 0 & R_s \end{bmatrix} \text{ and } [R_r] = \begin{bmatrix} R_r & 0 & 0 \\ 0 & R_r & 0 \\ 0 & 0 & R_r \end{bmatrix} \text{ matrix of statoric and rotoric resistances by}$$

phase.

Machine flow equations are:

$$[\psi_s] = [L_s].[I_s] + [L_m].[I_r] \tag{II.4}$$

$$[\psi_r] = [L_r].[I_r] + [L_m]^T.[I_s] \tag{II.5}$$

With:

$$[L_s] = \begin{bmatrix} L_{is} & M_{ss} & M_{ss} \\ M_{ss} & L_{is} & M_{ss} \\ M_{ss} & M_{ss} & L_{is} \end{bmatrix} \text{ is the stator leak induction matrix.}$$

$$[L_r] \begin{bmatrix} L_{ir} & M_{rr} & M_{rr} \\ M_{rr} & L_{ir} & M_{rr} \\ M_{rr} & M_{rr} & L_{ir} \end{bmatrix} \text{ is the rotor leak induction matrix.}$$

L_{is} and L_{ir} are the induction of stator phase and rotor phase, M_{ss} and M_{rr} are the mutual inductions between two stator phases and two rotor phases,

$$[L_m] = L_{sr}. \begin{bmatrix} \cos(\theta) & \cos(\theta + \frac{2\pi}{3}) & \cos(\theta - \frac{2\pi}{3}) \\ \cos(\theta - \frac{2\pi}{3}) & \cos(\theta) & \cos(\theta + \frac{2\pi}{3}) \\ \cos(\theta + \frac{2\pi}{3}) & \cos(\theta - \frac{2\pi}{3}) & \cos(\theta) \end{bmatrix} \text{ is the matrix of cyclic mutual}$$

inductions between the stator and the rotor.

From equations (II.2) (II.3) (II.4) (II.5), we obtain the followings expressions:

$$[V_s] = [R_s][I_s] + [L_s]\frac{d}{dt}[I_s] + \frac{d}{dt}\{[L_m][I_r]\} \tag{II.6}$$

$$[V_r] = [R_r][I_r] + [L_r]\frac{d}{dt}[I_r] + \frac{d}{dt}\{[L_m]^T[I_s]\} \tag{II.7}$$

II.3.3 Representation of DFIG in dq-coordinates

Park's transformation is used in DFIG modelling to simplify the complicated equations of the generator by transforming the three-phase stator and rotor quantities into a two-phase rotating reference frame, reducing the complexity of the model [38].
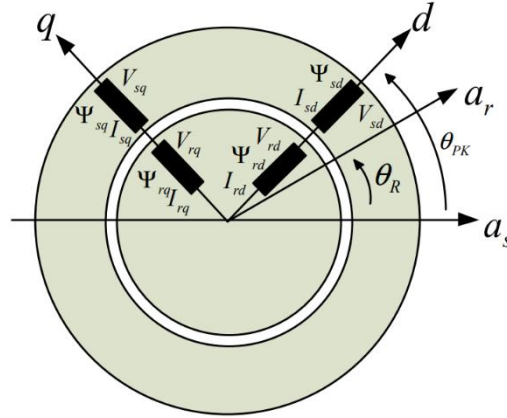
Figure II.9: representation of the DFIG in the biphasic reference

We next utilize the Park transformation provided by the rotation matrix P, to transform the variables of the (a-b-c) reference to the axes of the rotating (d-q) reference.

$$P = \sqrt{\frac{2}{3}} \begin{bmatrix} \cos(\theta) & \cos\left(\theta - \frac{2\pi}{3}\right) & \cos\left(\theta + \frac{2\pi}{3}\right) \\ -\sin\theta & -\sin\left(\theta - \frac{2\pi}{3}\right) & -\sin\left(\theta + \frac{2\pi}{3}\right) \\ \frac{1}{\sqrt{2}} & \frac{1}{\sqrt{2}} & \frac{1}{\sqrt{2}} \end{bmatrix} \tag{II.8}$$

θ_{PK} is the PARK transformation angle.

For stator quantity:

$$P(\theta_{PK})_S = \sqrt{\frac{2}{3}} \begin{bmatrix} \cos\theta_{PK} & \cos\left(\theta_{PK} - \frac{2\pi}{3}\right) & \cos\left(\theta_{PK} + \frac{2\pi}{3}\right) \\ \sin\theta_{PK} & -\sin\left(\theta_{PK} - \frac{2\pi}{3}\right) & -\sin\left(\theta_{PK} + \frac{2\pi}{3}\right) \end{bmatrix} \tag{II.9}$$

For rotor quantity:

$$P(\theta_{PK})_R = \sqrt{\frac{2}{3}} \begin{bmatrix} \cos(\theta_{PK} - \theta_R) & \cos\left(\theta_{PK} - \theta_R - \frac{2\pi}{3}\right) & \cos\left(\theta_{PK} - \theta_R + \frac{2\pi}{3}\right) \\ \sin(\theta_{PK} - \theta_R) & -\sin\left(\theta_{PK} - \theta_R - \frac{2\pi}{3}\right) & -\sin\left(\theta_{PK} - \theta_R + \frac{2\pi}{3}\right) \end{bmatrix} \tag{II.10}$$

The machine's voltage and flow equations in the diphase reference thus become:

$$\begin{cases} V_{ds} = R_s i_{ds} + \dot{\varphi}_{ds} - \omega_s \varphi_{qs} \\ V_{dr} = R_r i_{dr} + \dot{\varphi}_{dr} - \omega_r \varphi_{qr} \end{cases} \tag{II.11}$$

$$\begin{cases} V_{qs} = R_s i_{qs} + \dot{\varphi}_{qs} + \omega_s \varphi_{ds} \\ V_{qr} = R_r i_{qr} + \dot{\varphi}_{qr} + \omega_r \varphi_{dr} \end{cases}$$

$$\omega_s = \omega_{PK} \quad and \quad \omega_r = \omega_{PK} - \omega_R$$

$$\begin{cases} \varphi_{ds} = L_s i_{ds} + L_m i_{dr} \\ \varphi_{dr} = L_r i_{dr} + L_m i_{ds} \end{cases}$$

$$\begin{cases} \varphi_{qs} = L_s i_{qs} + L_m i_{qr} \\ \varphi_{qr} = L_r i_{qr} + L_m i_{qs} \end{cases}$$

(II.12)

With:

R_s, R_r, L_s, L_r and L_m are respectively the statoric and rotoric resistors and inductions and the mutual induction.

V_{ds}, V_{qs}, V_{dr}, V_{qr}, i_{ds}, i_{qs}, i_{dr}, i_{qr}, φ_{ds}, φ_{qs}, φ_{dr} and φ_{qr} are, respectively, the rotoric and statoric voltages, currents, and flows direct and quadrature components.

The electromagnetic torque can be expressed by different equations [38]:

$$T_{em} = P(\varphi_{ds} i_{qs} - \varphi_{qs} i_{ds}) \text{ or } \quad T_{em} = P(\varphi_{qr} i_{rd} - \varphi_{rd} i_{rq}) \tag{II.13}$$

The following relation defines the expressions of the statoric and rotoric active and reactive powers [38]:

$$\begin{cases} P_s = V_{ds} i_{ds} + V_{qs} i_{qs} \\ Q_s = V_{qs} i_{ds} - V_{ds} i_{qs} \end{cases} \tag{II.14}$$

And

$$\begin{cases} P_r = V_{dr} i_{dr} + V_{qr} i_{qr} \\ Q_r = V_{qr} i_{dr} - V_{dr} i_{qr} \end{cases} \tag{II.15}$$

II.3.4 Double fed induction generator equivalent scheme

The equations of the stator and rotor flows in the 'dq0' plan are given by the equations as follow. To build the equivalent model of the DFIG, new variables are defined from the equations (II.12), we put $L_s = L_{ls} + L_m \ and \ L_r = L_{lr} + L_m$ [37]:

$$\varphi_{ds} = L_s i_{ds} + M i_{dr} = (L_{ls} + L_m) i_{ds} + L_m i_{dr} = L_{ls} i_{ds} + L_m i_m \tag{II.16}$$

$$\varphi_{qs} = L_s i_{qs} + L_m i_{qr} = (L_{ls} + L_m) i_{qs} + L_m i_{qr} = L_{ls} i_{qs} + L_m i_m \tag{II.17}$$

$$\varphi_{dr} = L_r i_{dr} + L_m i_{ds} = (L_{lr} + L_m) i_{dr} + L_m i_{ds} = L_{lr} i_{dr} + L_m i_m \tag{II.18}$$

$$\varphi_{qr} = L_r i_{qr} + L_m i_{qs} = (L_{lr} + L_m) i_{qr} + L_m i_{qs} = L_{lr} i_{qr} + L_m i_m \tag{II.19}$$

The DFIG equivalent scheme is given in the following configuration [37]:
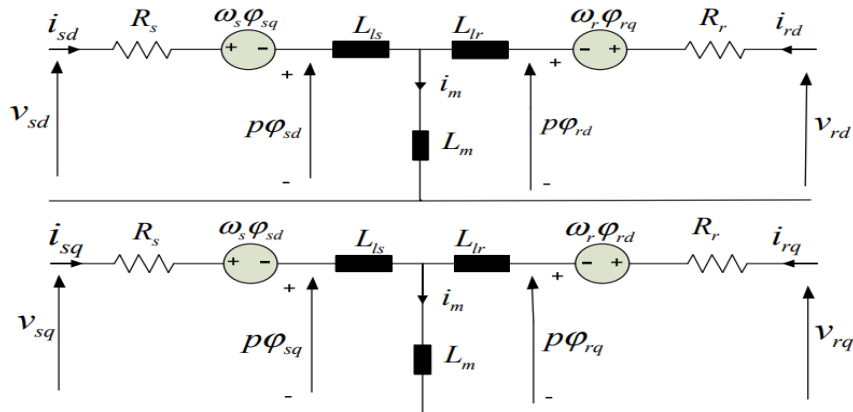
Figure II.10: Equivalent scheme of the machine in the 'dq' plan

II.4 Conclusion

This chapter provided a depth look at the modelling and representation of the Double Fed Induction Generator (DFIG) used in wind turbine systems. We began by introducing the DFIG and discussing the various types of generators used in wind turbines.

The core of the chapter focused on the modelling of the DFIG itself. We derived the DFIG model in both the abc-coordinate system and the dq-coordinate system. The abc-coordinate model captures the three-phase nature of the stator and rotor windings, while the dq-coordinate model simplifies the analysis by transforming the variables to a synchronous rotating reference frame. The DFIG equivalent circuit scheme was presented, based on the equations of the stator and rotor flows which clearly shows the power flow between the stator and rotor.

After the modelling of the DFIG, a control strategy of this latter must be introduced to understand and control the behaviour of the generator in wind conversion system to integrate it with the grid.

Chapter III

Vector control of DFIG

III.1 Introduction

A double fed induction generator is an induction machine, which both stator and rotor coil is connected to a source, thus refers to double fed [39]. As mentioned in previous chapter, in wind turbine system, the stator of the DFIG is connected to the grid and the rotor is connected in the back-to-back converters, the power flow within the stator side is unidirectional, whereas the rotor power flow is bidirectional.

Conventional DFIG control systems are usually defined in the synchronous d–q frame fixed to either the stator voltage or the stator flux, and it requires complex transformation of voltages, currents and control outputs across the stationary and the synchronous reference frames [40]. This traditional method necessitates precise parameters of machine including mutual inductance, resistance and inductance for both rotor and stator. The performance and stability of the system decreases, when the values used in the control system and the real machine parameters are different.

After the modelling of DFIG in previous chapter, we are interested in the field oriented control FOC of the active and reactive stator powers of the DFIG, applied to the wind system.

III.2 Overview of vector control strategy

Vector control or field-oriented control (FOC), is the most widely used techniques for the control of electrical machines. The base of it is a control law leading to an adjustment characteristic similar to that of a separately excited DC machine which can be controlled in a decoupled manner. The technique of the vector control introduced by Blaschk in 1972 is a revolution for control machines, for the vector control of the double-fed induction generator (DFIG), it will be a question of controlling the exchanges of energy and in particular the transfers of active and reactive power sent on the network [41]. Most DC drives have been replaced by AC machines because of this control method and the development of digital systems, allowing for more efficient speed adjustment

III.3 The principle of vector control

The basic idea of vector control is to control the asynchronous machine as an independent excitation DC machine where there is a natural decoupling between the excitation current which creates the flux and the current of a leading which provides electromagnetic torque [41]. This method is based on the transformation of the electrical variables of the machine into a reference

that rotates with the flow vector. In order to obtain a control similar to that of the DC machine with separate excitation. i_{rd} is analogous to the current of excitation, while the current i_{rq} is analogous to the induction current. Therefore, the two components are mutually decoupled, it's based on conventional regulators (proportional, integral and derivative).

III.4 Vector Control Variants

The field-oriented control applied to electric motors, is used to obtain the desired mode of operation by optimally positioning the current vectors and the resulting flux vectors.
Many variants of this command have been presented, which can be classified as follow [42]:

According to the source of energy:
-Voltage control;
-Current control.

Following the desired operations for the flux:
- Vector control of rotor flux;
- Stator flux vector control;
- Vector control of air gap flux (or magnetic flux).

Following the determination of the position of the flow:
- Direct by measuring or observing the flow vector (module, phase);
- Indirect by controlling the sliding frequency.

III.5 Vector Control of double fed induction generator

The expression of the electromagnetic torque of the DFIG makes it feasible to take consideration the asynchronous machine as a mechanical association of two DC machines, which allows to better interpret the coupling problem, between the magnitudes of the two axes, direct and quadrature.
Torque equation of separately excited DC machine in the absence of saturation is given by [43]:

$$T_{em} = K_a . \psi_f(I_f) . I_a \qquad \text{(III.1)}$$

Where: K_a is constant, ψ_f is field flux, I_f is excitation current and I_a is armature current.

By nature of construction in Figure III.1, the armature circuit and field circuit are isolated. There is no electrical connection in between, only some magnetically coupling exists. So, in armature side, the armature current and in field side, the field current can be controlled separately [43].
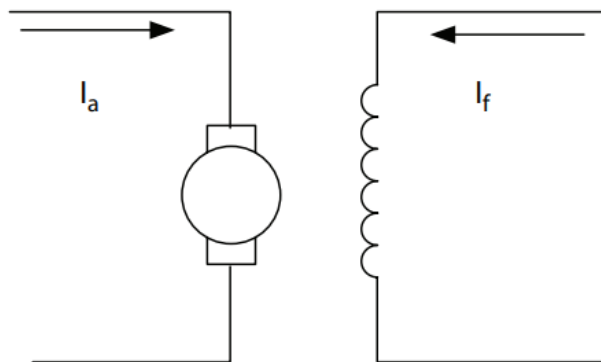
Figure III.1: Equivalent circuit of separately excited DC machine

According to expression (III.1) and figure (III.1), the flux depends on the excitation current. So, if the flux is constant the control of the torque is done only by the current I_a. Therefore, the production of the torque and the creation of the flux are independent.

The application of vector control on DFIG consists of achieving a decoupling between the quantities generating the torque and the flux. To do this, the flux can be adjusted by a component of the stator or rotor current i_{sd} or i_{rd} , and the torque by the other component (i_{sq} or i_{rq}).

Thus, the dynamics of the DFIG will be reduced to that of a direct current machine. This method can be schematized as follows:
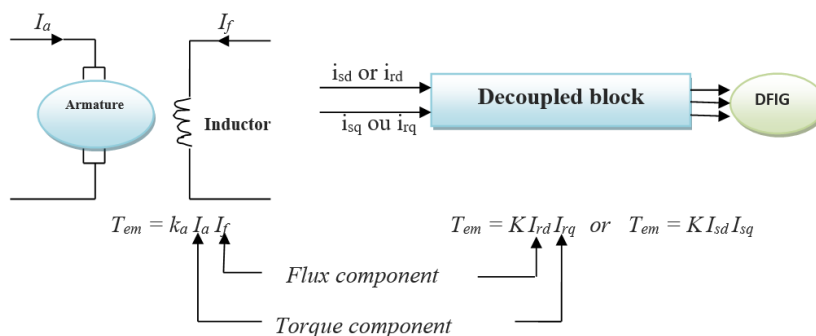
Figure III.2: Analogy between the vector control of a DFIG and the control of an DC motor.

III.6 Different reference frames

In order to simplify the control of powers, we can choose the reference frame axes according to one of the machine fluxes:

Rotor flux: $\varphi_{dr} = \varphi_r$

Stator flux: $\varphi_{ds} = \varphi_s$

Air gap flux: $\varphi_{dg} = \varphi_g$

In this study, we are interested in vector control by orientation of the stator flux [44].

III.7 Stator flux-oriented control structure and modelling

In a SFOC reference frame, where the d axis is attached to the stator flow space vector, the following characteristics are obtained [45]

$$\begin{cases} \varphi_{ds} = \varphi_s \\ \varphi_{qs} = 0 \end{cases} \tag{III.2}$$

This allows to obtain an expression of the torque, in which the two stator or rotor current components intervene; the first produces the flux and the other produces the torque.

the principle of the vector control consists to orient the stator flux vector to the direct (d-axis) of the rotating reference frame as shown in figure

(A) : phase statorique
(a) : phase rotorique
(dq): repère de park
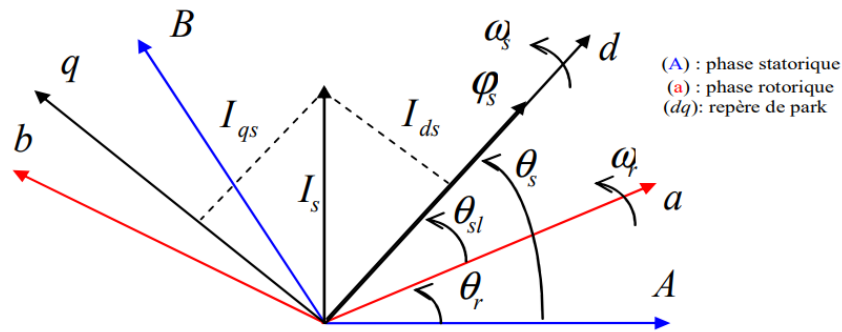
Figure III.3: Flux orientation [46]

Let's review the machine's voltage and flows equations (II.11) (II.12) in the diphase reference

$$\begin{cases} V_{ds} = R_s i_{ds} + \dot{\varphi}_{ds} - \omega_s \varphi_{qs} \\ V_{dr} = R_r i_{dr} + \dot{\varphi}_{dr} - \omega_r \varphi_{qr} \end{cases} \tag{III.3}$$

$$\begin{cases} V_{qs} = R_s i_{qs} + \dot{\varphi}_{qs} + \omega_s \varphi_{ds} \\ V_{qr} = R_r i_{qr} + \dot{\varphi}_{qr} + \omega_r \varphi_{dr} \end{cases}$$

$$\begin{cases} \varphi_{ds} = L_s i_{ds} + L_m i_{dr} \\ \varphi_{dr} = L_r i_{dr} + L_m i_{ds} \end{cases} \tag{III.4}$$

$$\begin{cases} \varphi_{qs} = L_s i_{qs} + L_m i_{qr} \\ \varphi_{qr} = L_r i_{qr} + L_m i_{qs} \end{cases}$$

According to (III.2), these equations can be simplified as follows

$$\begin{cases} V_{ds} = R_s i_{ds} \\ V_{dr} = R_r i_{dr} + \dot\varphi_{dr} - \omega_r \varphi_{qr} \end{cases}$$ (III.5)

$$\begin{cases} V_{qs} = R_s i_{qs} + \omega_s \varphi_s \\ V_{qr} = R_r i_{qr} + \dot\varphi_{qr} + \omega_r \varphi_{dr} \end{cases}$$

In the same way as for tensions, the flows equations become

$$\begin{cases} \varphi_{ds} = L_s i_{ds} + L_m i_{dr} = \varphi_s \\ \varphi_{qs} = L_s i_{qs} + L_m i_{qr} = 0 \end{cases}$$ (III.6)

From equation (III.6) we obtain

$$\begin{cases} i_{ds} = \dfrac{\varphi_s - L_m i_{dr}}{L_s} \\ i_{qs} = \dfrac{-L_m i_{qr}}{L_s} \end{cases}$$ (III.7)

The statoric current obtained in (III.7), will be replaced in the expression of electromagnetic torque expression (II.13), which gives

$$T_{em} = P(\varphi_{ds} i_{qs} - \varphi_{qs} i_{ds}) = -P\frac{L_m i_{qr}}{L_s}\varphi_s$$ (III.8)

If we ignore the stator resistance R_s, which is a frequently accepted assumption for medium and high power generators used in the production of wind energy, the machine voltage equations are reduced to the following form [44].

$$\begin{cases} V_{ds} = 0 \\ V_{dr} = R_r i_{dr} + \dot\varphi_{dr} - \omega_r \varphi_{qr} \end{cases}$$ (III.9)

$$\begin{cases} V_{qs} = V_s = \omega_s \varphi_s \\ V_{qr} = R_r i_{qr} + \dot\varphi_{qr} + \omega_r \varphi_{dr} \end{cases}$$

V_s: the voltage of the electrical grid.

In a two-phase reference frame, the statoric active and reactive powers (II.14) of an DFIG are written together

$$\begin{cases} P_s = V_{ds} i_{ds} + V_{qs} i_{qs} \\ Q_s = V_{qs} i_{ds} - V_{ds} i_{qs} \end{cases}$$ (III.10)

According to the assumption of an oriented statoric flow, this system of equations can be simplified in the following form

$$\begin{cases} P_s = V_s i_{qs} \\ Q_s = V_s i_{ds} \end{cases} \tag{III.11}$$

By replacing the direct and quadrature statoric currents with their expressions (III.7) in the active and reactive power equations (III.12), we find

$$\begin{cases} P_s = -V_s \dfrac{L_m i_{qr}}{L_s} \\ Q_s = \dfrac{V_s^2}{\omega_s . L_s} - \dfrac{V_s . L_m}{L_s} . i_{dr} \end{cases} \tag{III.12}$$

The equations above have shown that, independent (decoupled) control of active power P is proportional to rotoric current of q-axis i_{qr} and reactive power Q is proportional to rotoric current of d-axis i_{dr} in SFOC. The constant $\dfrac{V_s^2}{\omega_s . L_s}$ is imposed by the network.

III.7.1 Relation between stator powers and rotor currents

By replacing the expressions for the stator currents (III.7) in the rotor flux equations we get:

$$\begin{cases} \varphi_{dr} = L_r i_{dr} + L_m \left(\dfrac{V_s}{\omega_s L_s} - \dfrac{L_m}{L_s} i_{dr} \right) \\ \varphi_{qr} = L_r i_{qr} + L_m (\dfrac{-M}{L_s} i_{qr}) \end{cases} \tag{III.13}$$

By taking i_{dr} as common factor, we obtain:

$$\begin{cases} \varphi_{dr} = (L_r - \dfrac{L_m^2}{L_s}) i_{dr} + \dfrac{M V_s}{L_s \omega_s} \\ \varphi_{qr} = (L_r - \dfrac{L_m^2}{L_s}) i_{qr} \end{cases} \tag{III.14}$$

We substitute the resulting expressions ((III.14) in the rotor voltage equations in d and q reference. Hence, we find:

$$\begin{cases} V_{dr} = R_r i_{dr} + (L_r - \dfrac{L_m^2}{L_s}) \dfrac{di_{dr}}{dt} - \dfrac{(\omega_s - \omega)}{\omega_s} . \omega_s (L_r - \dfrac{L_m^2}{L_s}) i_{qr} \\ V_{qr} = R_r i_{qr} + (L_r - \dfrac{L_m^2}{L_s}) \dfrac{di_{qr}}{dt} + \omega_s \left(L_r - \dfrac{L_m^2}{L_s} \right) i_{dr} + \dfrac{(\omega_s - \omega)}{\omega_s} . \omega_s \left(\dfrac{L_m V_s}{\omega_s L_s} \right) \end{cases} \tag{III.15}$$

We   take $g = \frac{(\omega_s - \omega)}{\omega_s}$ the   slip,   the   expressions   (III.15)   become

$$
\begin{cases}
V_{dr} = R_r\, i_{dr} + (L_r - \frac{Lm^2}{L_s})\frac{di_{dr}}{dt} - g.\omega_s\,(L_r - \frac{Lm^2}{L_s})i_{qr} \\
V_{qr} = R_r\, i_{qr} + (L_r - \frac{Lm^2}{L_s})\frac{di_{qr}}{dt} + \omega_s.g\left(L_r - \frac{Lm^2}{L_s}\right)i_{dr} + g.\omega_s\left(\frac{Lm V_s}{\omega_s L_s}\right)
\end{cases}
\tag{III.16}
$$

In steady state, the derivatives of the two-phase rotor currents disappear, we therefore write:

$$
\begin{cases}
V_{dr} = R_r\, i_{dr} - g.\omega_s\,(L_r - \frac{Lm^2}{L_s})i_{qr} \\
V_{qr} = R_r\, i_{qr} + \omega_s.g\left(L_r - \frac{Lm^2}{L_s}\right)i_{dr} + g.\omega_s\left(\frac{Lm V_s}{\omega_s L_s}\right)
\end{cases}
\tag{III.17}
$$

V_{dr} and V_{qr} are the two-phase components of the rotor voltages to be imposed on the machine to obtain the desired rotor currents.

The influence of the coupling terms between the two axes $\left(L_r - \frac{Lm^2}{L_s}\right)$ is minimal. An adequate synthesis of the regulators in the control loop will make can compensate them. The term $g.\omega_s\,(L_r - \frac{Lm^2}{L_s})$ represents an electromotive force dependent on the speed of rotation. Its influence is not negligible because it causes a lagging error. The system control must therefore take this error into account.

Using the Laplace transform on the rotor voltage equations (III.16), with **s: the Laplace operator**, we get:

$$
\begin{cases}
V_{dr}(s) = R_r\, I_{dr}(s) + (L_r - \frac{M^2}{L_s})\, s\, I_{dr}(s) - g\omega_s\,(L_r - \frac{M^2}{L_s})\, I_{qr}(s) \\
V_{qr}(s) = R_r\, I_{qr}(s) + (L_r - \frac{M^2}{L_s})\, s\, I_{qr}(s) + g\omega_s\left(L_r - \frac{M^2}{L_s}\right)I_{dr}(s) + g\omega_s\left(\frac{M V_s}{\omega_s L_s}\right)
\end{cases}
\tag{III.18}
$$

From the equation (III.18), we derive the expressions of the rotor currents in d and q axis:

$$
\begin{cases}
I_{dr}(s) = \dfrac{V_{dr}(s) + g.\omega_s\left(L_r - \frac{Lm^2}{L_s}\right)I_{qr}(s)}{R_r + \left(L_r - \frac{Lm^2}{L_s}\right)s} \\[4mm]
I_{qr}(s) = \dfrac{V_{qr}(s) - g\omega_s\left(L_r - \frac{Lm^2}{L_s}\right)I_{dr}(s) - g\omega_s\left(\frac{Lm V_s}{\omega_s L_s}\right)}{R_r + \left(L_r - \frac{Lm^2}{L_s}\right)s}
\end{cases}
\tag{III.19}
$$

We replace the expressions obtained ((III.19) in the stator power equations (III.12), we have:

$$\begin{cases} P_s = -V_s \dfrac{L_m}{L_s} \left(\dfrac{V_{qr}(s) - g\left(L_r - \frac{L_m^2}{L_s}\right) I_{dr}(s) - g\,\omega_s \left(\frac{L_m\,V_S}{\omega_s\,L_S}\right)}{R_r + \left(L_r - \frac{L_m^2}{L_s}\right) s} \right) \\[4mm] Q_s = \dfrac{V_s \varphi_s}{L_s} - \left(\dfrac{V_s\,L_m}{L_s} \;\; \dfrac{V_{dr}(s) + g\,\omega_s\,(L_r - \frac{M^2}{L_s})\,I_{qr}(s)}{R_r + \,(L_r - \frac{M^2}{L_s})\,s} \right) \end{cases} \qquad \text{(III.20)}$$

Equations (III.20) allow to build a block diagram of the electrical system to be regulated (figure III.4):
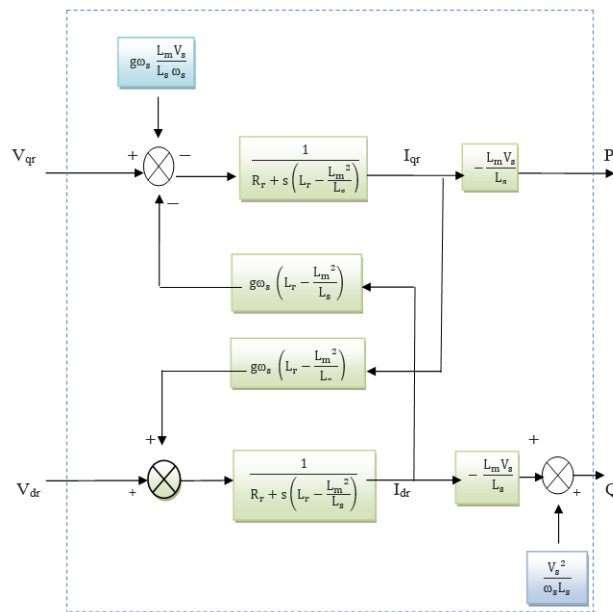
Figure III.4: Block diagram of the regulated system

In this diagram we can notice that the powers and the voltages are linked by transfer functions with first order. Because the value of the slip ''g'' is low and the influences of the coupling is weak, the d and q axes can be controlled separately. This will allow us to easily establish the vector control [47].

III.8 Field oriented control

The active power must make it possible to keep the power coefficients of the wind turbine optimal. There are two ways to perform the control power of this machine:

Direct field-oriented control DFOC: This type of control consists in neglecting the terms of coupling and setting up an independent regulator on each axis to control active and reactive

power independently [41]. This one called the "direct method" because the power regulators directly control the machine's rotor tensions.

Indirect field oriented IFOC: Unlike the first method, this method is to consider the coupling terms and compensate them performing a system with two loops to control the powers and rotor currents. That why it's called indirect method [47].

The advantage of the direct method is that its simple algorithm, on the other hand the indirect method controls the rotor currents, which allows to protect the machine by limiting its currents, the amin drawback is complex to implement.

III.8.1 Direct method

Using the link between, on the one hand, the active power and the voltage V_{qr}, and on the other hand the reactive power and the voltage V_{dr}, we present the regulation of the active and reactive powers of the machine.

III.8.1.1 Implementation of regulation

We neglect the coupling terms between the two control axes due to the low slip value. We then obtain a vector control with a single regulator per axis, PI (Proportional–integral) is the regulator used to control active and reactive powers. presented in the figure (III.5):
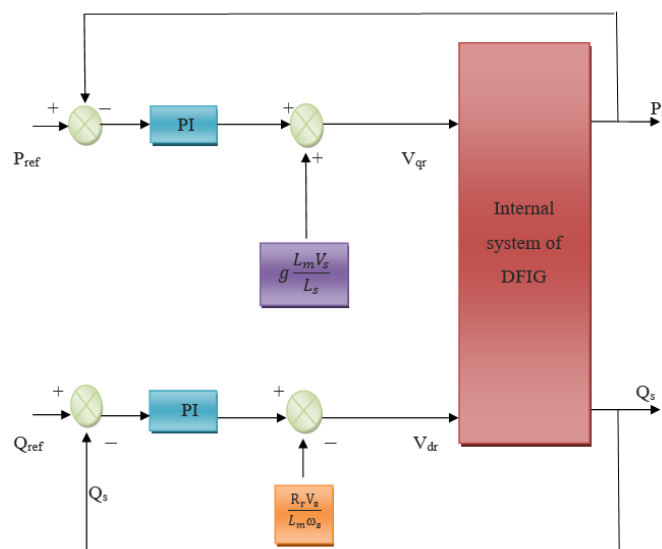
Figure III.5: Direct Field Oriented Control

III.8.1.2 PI regulator

Integral Proportional Controller PI, used to control the DFIG, it is simple and fast to implement while offering acceptable performance. Proportional action is used to regulate the speed of the dynamics of the system, while integral action eliminates the gap between the set quantity and the quantity to be enslaved and that was the reason why it has retained our attention for a global study of the system [41].

Figure (III.6) shows part of the system looped and corrected by a PI regulator whose function is transfer is of the form [46]

$$F_T(s) = k_p + \frac{k_i}{s} \tag{III.21}$$

k_p : is the proportionality coefficient;

k_i : is the integration coefficient;

Corresponding to the two regulators used in the figure (III.5):
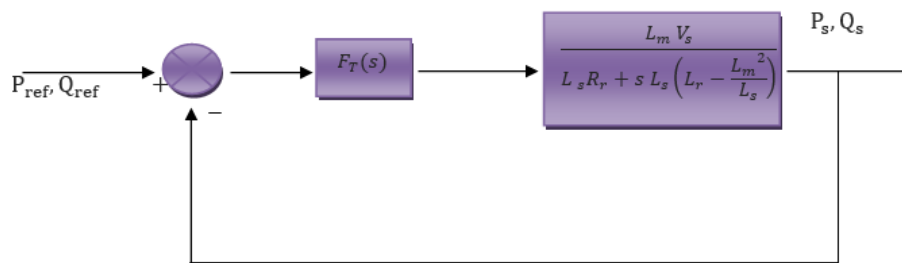
Figure III.6: System regulated by a PI regulator

The transfer function of the open loop system is given by:

$$OLTF = \frac{s + \frac{K_i}{K_p}}{\frac{s}{K_p}} \cdot \frac{\frac{L_m V_S}{L_S \left(L_r - \frac{L_m^2}{L_S}\right)}}{s + \frac{R_r}{\left(L_r - \frac{L_m^2}{L_S}\right)}} \tag{III.22}$$

We choose the pole compensation method for the synthesis of the regulator in order to eliminate the zero of the transfer function. This leads us to the following equality:

$$\frac{K_i}{K_p} = \frac{R_r}{(L_r - \frac{Lm^2}{L_s})} \tag{III.23}$$

By performing the compensation, we obtain the following OLTF:

$$OLTF = \frac{K_p \dfrac{L_m V_s}{L_s (L_r - \frac{Lm^2}{L_s})}}{s} \tag{III.24}$$

The closed loop transfer function is then expressed by:

$$CLTF = \frac{FTBO}{1+FTBO} = \frac{K_p \dfrac{L_m V_s}{L_s (L_r - \frac{Lm^2}{L_s})}}{s + K_p \dfrac{L_m V_s}{L_s (L_r - \frac{Lm^2}{L_s})}} \tag{III.25}$$

$$CLTF = \frac{1}{1+ s.\tau_r} \tag{III.26}$$

From (III.25), (III.26):

$$\tau_r = \frac{1}{K_p} . \frac{L_s (L_r - \frac{Lm^2}{L_s})}{L_m V_s} \tag{III.27}$$

τ_r is the real time constant of the system, and will be chosen during the simulation in order to offer the best compromise between performances.

We can express the gains of the correctors as a function of the machine parameters and the time constant as follows

$$K_p = \frac{1}{\tau_r} . \frac{L_s (L_r - \frac{Lm^2}{L_s})}{L_m V_s} \tag{III.28}$$

By replacing equation (III.28) in equation (III.23) we obtain:

$$K_i = \frac{1}{\tau_r} . \frac{R_r L_s}{L_m V_s} \tag{III.29}$$

It is obvious that the pole compensation method is not the only valid method for the synthesis of the PI regulator, we choose to use it because of its speed [46].

III.8.2 Indirect method

By keeping the same assumptions on the stability of the network (V_s constant). And combining the different equations for fluxes, rotor voltages, currents and powers, we can express the voltages as a function of the powers [48].

We start from the stator power as a function of the rotor currents (III.20) and then from the expressions of the rotor voltages as a function of the rotor currents (III.17), we obtain:

$$\begin{cases} V_{dr} = g\,\omega_s\, \dfrac{(L_r - \frac{L_m^2}{L_s})}{\frac{V_s L_m}{L_s}}\,.P_s - \left(\dfrac{R_r + (L_r - \frac{L_m^2}{L_s})}{\frac{V_s L_m}{L_s}}\, .\, s \right) Q_s + \left(\dfrac{R_r V_s}{\omega_s L_m} + \left(L_r - \dfrac{L_m^2}{L_s} \right) \dfrac{V_s}{\omega_s L_m} s \right) \\[2em] V_{qr} = -\left(\dfrac{R_r + \left(L_r - \frac{L_m^2}{L_s} \right)}{\frac{V_s L_m}{L_s}}\, s \right).P_s - g\,\omega_s\, \dfrac{(L_r - \frac{L_m^2}{L_s})}{\frac{V_s L_m}{L_s}}\, Q_s + g\,\omega_s \left(L_r - \dfrac{L_m^2}{L_s} \right) \end{cases} \tag{III.29}$$

III.8.2.1 Control without power loop

The regulators of this control structure are calculated in the same way as for direct control. They are identical for each axis. In order to guarantee good stability of the system, we introduce a loop for regulating the rotor currents, whose instructions are directly deduced from the power values, which we want to impose on the machine. We thus establish the regulation system of the in figure (III.6) [48].

Figure III.7: Block diagram of indirect control without power loop

III.8.2.2 Control with power loop

In order to ameliorate the previous control, we introduce an additional regulation loop at the power level, in order to eliminate the static error while preserving the dynamics of the system. We can clearly distinguish two regulation loops for each axis, one controlling the current, and the other, the power [49].
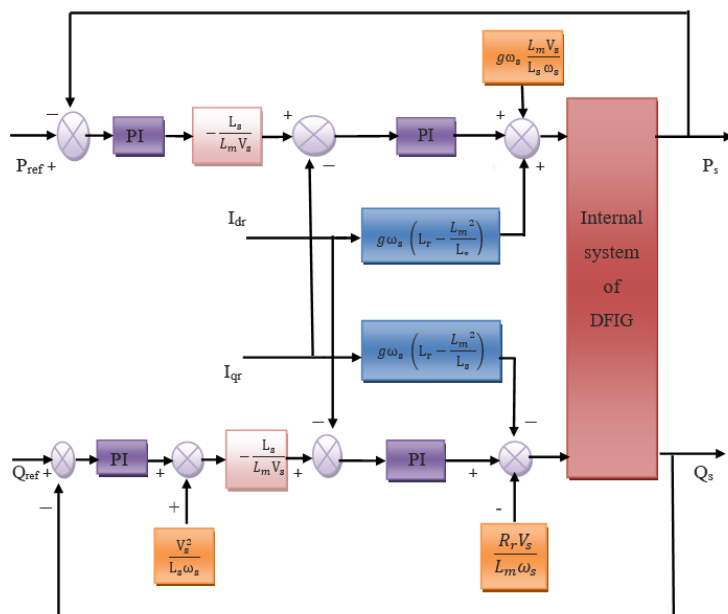
Figure III.8: Block diagram of indirect control with power loop

III.9 Conclusion

This chapter presents a comprehensive overview of vector control or field-oriented control, the chapter highlights the importance of vector control in maintaining the stability and efficiency of DFIG-based wind turbines. A suitable model is used, allows the control of active and reactive powers through the regulation of rotor voltages. Thus, three control methods were adopted, a direct mode in which powers are measured and compared to their references using a PI type regulator, another called indirect method where the rotor currents are used to control the powers, a third method has the supplement of improving the previous command by adding a power loop at the power level. The control of grid powers will present in the coming chapter.

Chapter IV

Grid side converter control

IV.1 Introduction

Grid side converter control of a doubly fed induction generator in wind turbines has two essential roles. It is responsible for the DC bus voltage adjustment regardless of the amplitude and direction of the flow of rotor power, and it regulates the power factor at the point of connection with the grid. Additionally, it controls the flow of active and reactive power to and from the grid [50].

In this chapter, we present the grid side modelling including the filter and DC connection with its algorithm control, then simulation and results that show the control of the active and reactive power transfer between the grid and GSC.

IV.2 Modelling of grid side converter

This part focuses on the modelling of the connection of the GSC, with the grid via the RL filter. The topology of grid GSC is shown in Figure IV.1 which illustrates the entire connection to the power grid, consisting of the DC bus, the GSC and the filter [50].
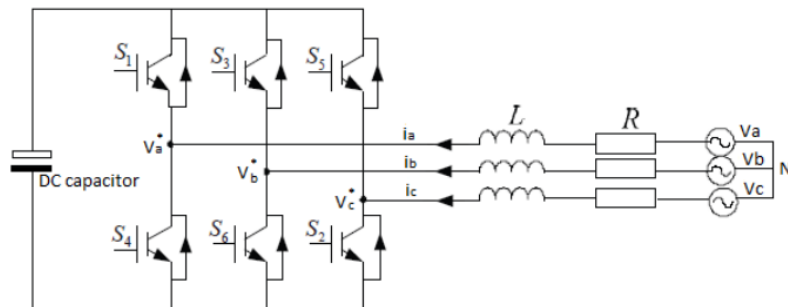
Figure IV.1: The topology of grid-side converter [51]

Where V_a^*, V_b^* and V_c^* are the input voltages of the converter, i_a, i_b and i_c are the input currents, R and L are resistance and inductance of filter respectively, V_a, V_b and V_c are three-phase grid voltage.

IV.2.1 DC Bus modelling

The power flow and the currents in the DC bus shown in Figure IV.2 are expressed by

$$P_{cap} = P_{GSC} - P_{MSC} \qquad\qquad (IV.1)$$

$$I_{cap} = I_{GSC} - I_{MSC} \qquad\qquad (IV.2)$$

Where P_{cap} and I_{cap} are the power absorbed by the capacitor and the current passing through the capacitor respectively. P_{GSC} and I_{GSC} are the power delivered by the GSC and current modulated by GSC respectively. P_{MSC} and I_{MSC} are the power absorbed by the MSC and current modulated by MSC respectively.
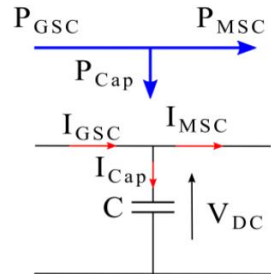
Figure IV.2: DC Link circuit [50]

The voltage at the terminals of the DC bus expression is obtained from the integration of the current circulating in the capacitor

$$\frac{dV_{dc}}{dt} = \frac{1}{C} i_{cap} \tag{IV.3}$$

From (IV.3), P_{cap} can be expressed by its linearized expression as follow

$$P_{cap} = V_{dc}.C.\frac{dV_{dc}}{dt} \tag{IV.4}$$

From equation (IV.1) and (IV.4) the DC bus voltage expression becomes

$$\frac{dV_{dc}}{dt} = \frac{1}{C}\frac{P_{GSC}-P_{MSC}}{V_{dc}} \tag{IV.5}$$

IV.2.2 Grid filter inverter modelling

According to Kirchhoff law applied to the circuit of figure below
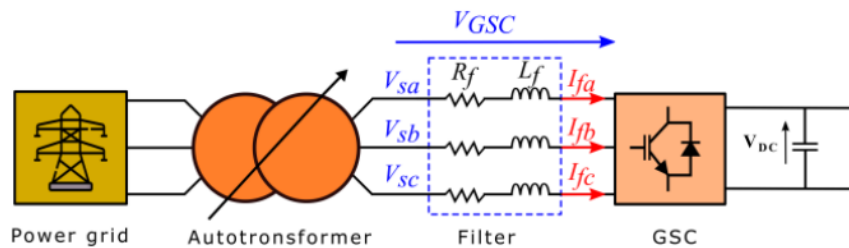
Figure IV.3: Scheme of the GSC inverter, the filter and the grid [50]

The phase voltages between the GSC and the grid can be expressed in the stationary abc reference frame as follows [38].

$$\left[V_{GSC_K}\right] = R_f.I_{f_K} + L_f\frac{dI_{f_K}}{dt} + V_{s_K} \tag{IV.6}$$

Where $K = a, b$ and c

We transform the previous model to the dq reference frame in order to apply the vector control principle, The GSC voltages will be expressed as follow

$$\begin{cases} V_{fd} = R_fI_{fd} + L_f\frac{dI_{fd}}{dt} - \omega_sL_fI_{fq} + V_{sd} \\ V_{fd} = R_fI_{fq} + L_f\frac{dI_{fq}}{dt} + \omega_sL_fI_{fd} + V_{sq} \end{cases} \tag{IV.7}$$

The active power and the reactive power of the GSC in the d-q reference frame are expressed by [52]

$$\begin{cases} P_{GSC} = V_{sd}I_{fd} + V_{sq}I_{fq} \\ Q_{GSC} = V_{sq}I_{fd} - V_{sd}I_{fq} \end{cases} \tag{IV.8}$$

IV.3 Control of the grid side converter

The principle of the control of the grid side converter performs the following two functions:
Control currents that flowing in the RL filter.
Control voltage of the DC bus [53].
The following figure (IV.4) describes GSC technique
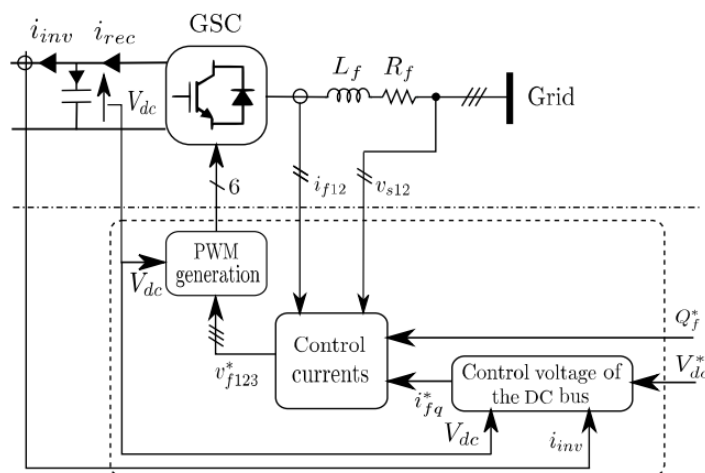
Figure IV.4: Principle of the control of the grid side converter [54]

IV.3.1 Control currents flowing in the RL filter

To control the GSC powers, we use a grid voltage orientated control (VOC). So, the grid voltage

vector Vs is hold on the q-axis which means [50]

$$\begin{cases} V_{sd} = 0 \\ V_{sq} = U_s \end{cases} \qquad (IV.9)$$

From the equation (IV.8) and according to (IV.9), we give the expression of the GSC powers in function of the grid side current as following

$$\begin{cases} P_{GSC} = U_s I_{fq} \\ Q_{GSC} = U_s I_{fd} \end{cases} \qquad (IV.10)$$

The model obtained allows the controlling of GSC active and reactive power independently each has its own regulator. The grid active power control depends on the quadrature current I_{fq} while the reactive power control depends on direct current I_{fd}. The GSC voltages which present the outputs of the current controller are given by the following expression [50]

$$\begin{cases} V_{fd} = R_f I_{fd} + L_f \dfrac{dI_{fd}}{dt} - \omega_s L_f I_{fq} \\ V_{fq} = R_f I_{fq} + L_f \dfrac{dI_{fq}}{dt} + \omega_s L_f I_{fd} + U_s \end{cases} \qquad (IV.11)$$

The control loop diagram of the GSC currents is shown in figure below
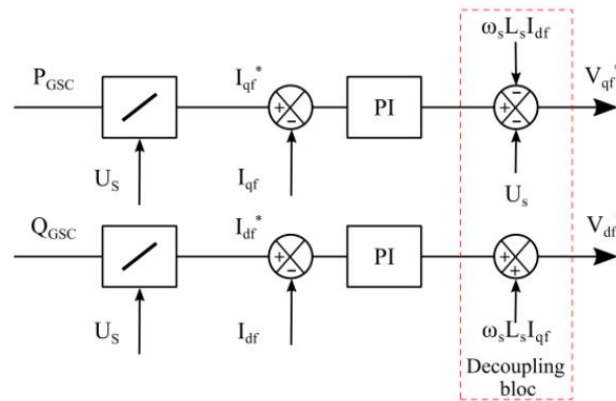
Figure IV.5: control loop diagram of currents flowing in the RL filter [50]

The error signal which is the difference between the measured value (I_{fq}, I_{fd}) and the reference value (I_{fq}^*, I_{fd}^*) as shown in the figure above, are fed in a PI controller. In conventional control systems, the reactive power reference is set to zero for a unity power factor. High power control

system performance is achieved by the integration of the decoupling block and precise controller parameter calculating.

IV.3.2 DC Bus control

we can express the powers put on the continuous bus by

$$\begin{cases} P_{GSC} = V_{dc}.I_{GSC} \\ P_{MSC} = V_{dc}.I_{MSC} \\ P_{cap} = V_{dc}.I_{cap} \end{cases} \tag{IV.12}$$

From the equation (IV.1) we get

$$P_{GSC} = P_{cap} + P_{MSC} \tag{IV.13}$$

Neglecting all the Joule losses (losses in the capacitor, the converter and the RL filter), we can write [54]

$$P_f \approx P_{GSC} = P_{cap} + P_{MSC} \tag{IV.14}$$

To regulate the DC bus voltage, it is possible by controlling the power P_{cap} in the capacitor by adjusting the power P_f.To achieve that, the P_{MSC} and P_{cap}^* powers must be known to determine reference value P_f^*. The reference power for the capacitor is connected to the reference current flowing through the capacitor as written

$$P_{cap}^* = V_{dc}.I_{cap}^* \tag{IV.15}$$

The control schema of the voltage at the terminals of the capacitor is given by the following figure IV.6 which shows that we can regulate the DC bus voltage using an external loop, based on a PI controller that generates the reference I_{cap}^* [54].
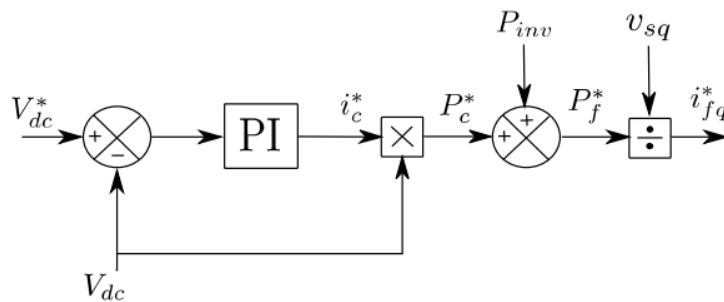
Figure IV.6: control schema of the voltage at the terminals of the capacitor [54]

IV.4 Simulation and results

The wind power system contains the turbine, DFIG, back-to-back converter and the grid was simulated under the environment MATLAB-SIMULINK.

The strategy for active and reactive power control in DFIG wind turbine is SFO vector control. The design comprises of two converters. One is utilized for RSC and another is utilized for GSC. The control of DFIG is accomplished by controlling the RSC and the GSC. The fundamental goal of the RSC is to controls the dynamic (Ps) and responsive power (Qs). The point of the GSC is to keep up the DC-link voltage (Vdc) as steady. by managing rotor streams in direct and quadrature references, the control of the active power (Ps) and reactive power (Qs) is accomplished and additionally rotor speed of the generator is controlled.

The different parameters used in the simulation are given in the following table:

Table IV.1: DFIG parameters [38]

Parameter	Symbol	Value
Nominal power	Pn	1.5 MW
Rotational speed	w	190 rad/s
Generator rated voltage	Vg	690V
Stator phase resistance	Rs	0.0120 Ω
Rotor phase resistance	Rr	0.0210 Ω
Stator phase inductance	Ls	$2.0372 * 10^{-4}$ H
Rotor phase inductance	Lr	$1.7507 * 10^{-4}$ H
Mutual inductance	Lm	0.0350 H
Friction coefficient	fg	$0.0024\ N.ms^{-1}$
Number of pole pairs	p	2
Rotor inertia moment	Jr	$0.3125\ Kg.m^2$

Table IV.2: wind turbine parameters

Parameter	Symbol	Value
Nominal power	*Pn*	1.5 MW
Gearbox ratio	*G*	70
Turbine inertia moment	*Jt*	$1\,Kg.m^2$

The simulations of the whole system were performed with MATLAB/Simulink using the parameters of the wind system in appendix, the DC bus reference voltage, denoted V_{dc} is set at 1200V. The reactive power reference Q_f is set to 0 VAR, which guarantees a unitary power factor at the GSC connection to the grid. After modelling the whole system, we have adopted the stator direct field-oriented control.

IV.4.1 First simulation

The first simulation is a DFIG wind turbine with voltage-oriented control of three phase PWM rectifier, the results of the active and reactive powers and FFT (Fast Fourier Transform) analysis current are given in the following figures:
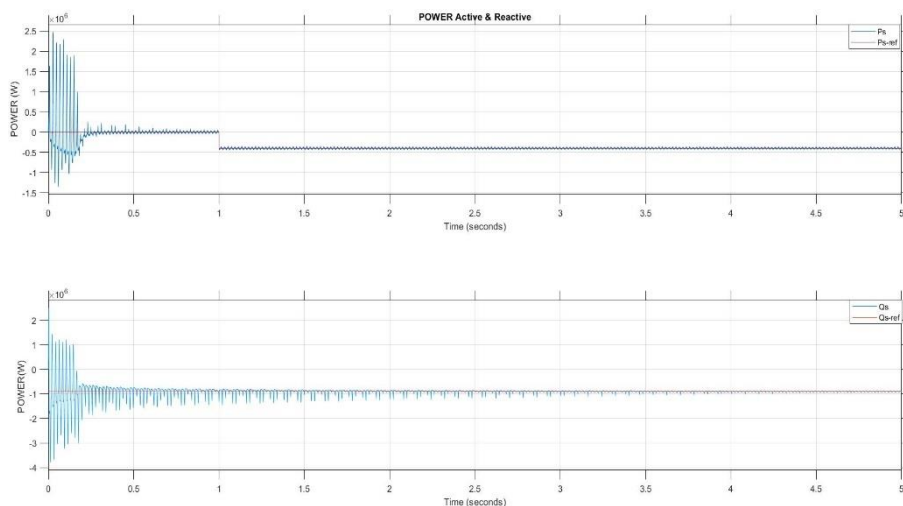
Figure IV.7: Stator active and reactive power with VOC configuration
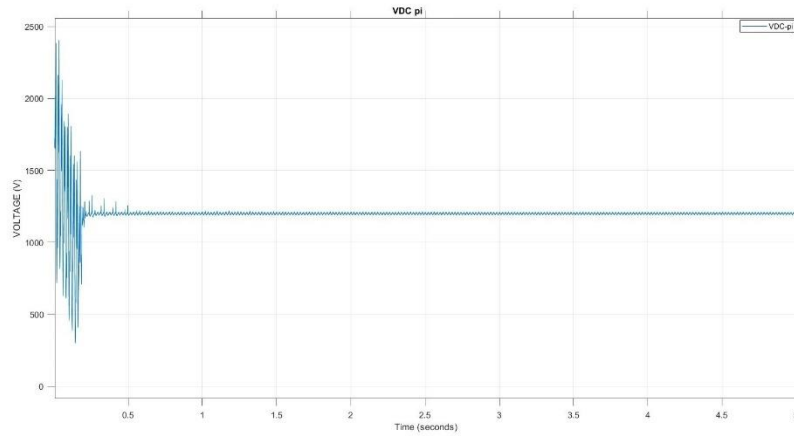
Figure IV.8: DC link voltage
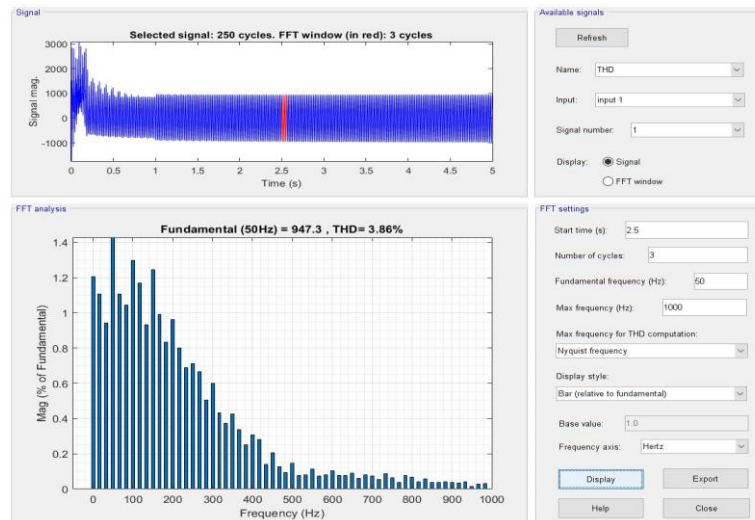
Figure IV.9: Spectrum analysis of the Total Harmonic Distortion for the Current Stator Is

IV.4.2 Discussion and interpretation

We can see in figure IV.7 that the we can observe that the control technique allows perfect decoupling between the two components of active and reactive stator power in the steady-state and follow their reference exactly, this is due to control of direct and quadrature components of the rotor current, when figure IV.8 shows that the DC bus voltage is perfectly regulated at 1200V. The harmonics in figure IV.9 appearing on the injected stator current Is to the grid are THD of 3.86% is relatively low, indicating that the signal mainly consists of the fundamental frequency with moderate harmonic contributions, a THD values below 5% are generally acceptable. That implies the wind energy provide the optimal electrical energy to the network.

The active power on the stator side is adjustable according to the network needs, negative which means that the network in this case is a receiver of the energy provided by the DFIG.

IV.4.3 Second simulation

The second simulation consists of DFIG wind turbine with direct power control of three phase PWM hysteresis rectifier, the results of the active and reactive powers and the FFT analysis of stator current are given in the following figures:
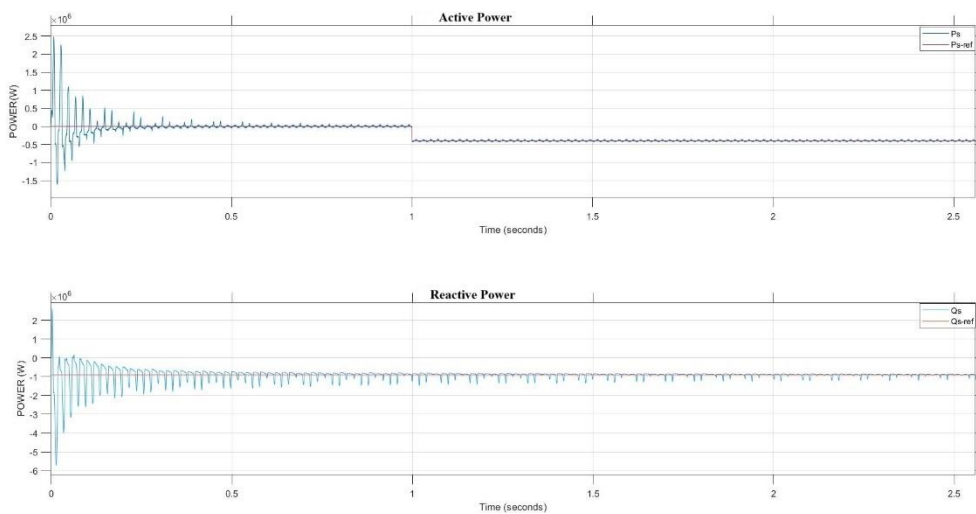
Figure IV.11: Stator active and reactive power with DPC configuration
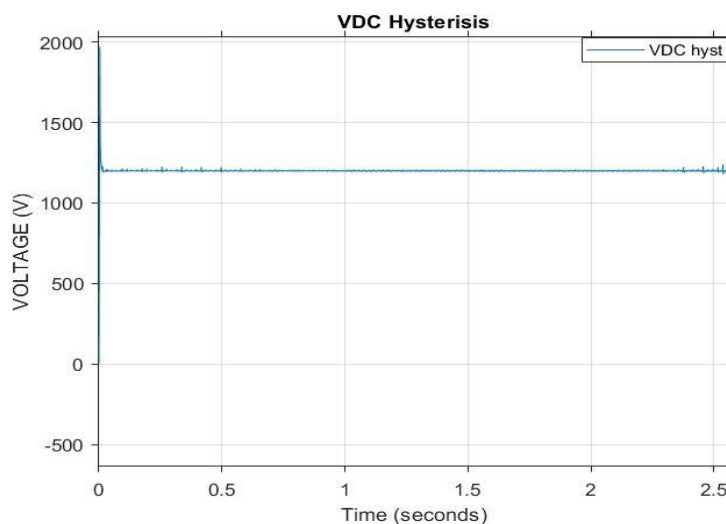
Figure IV.12: DC link voltage waveform
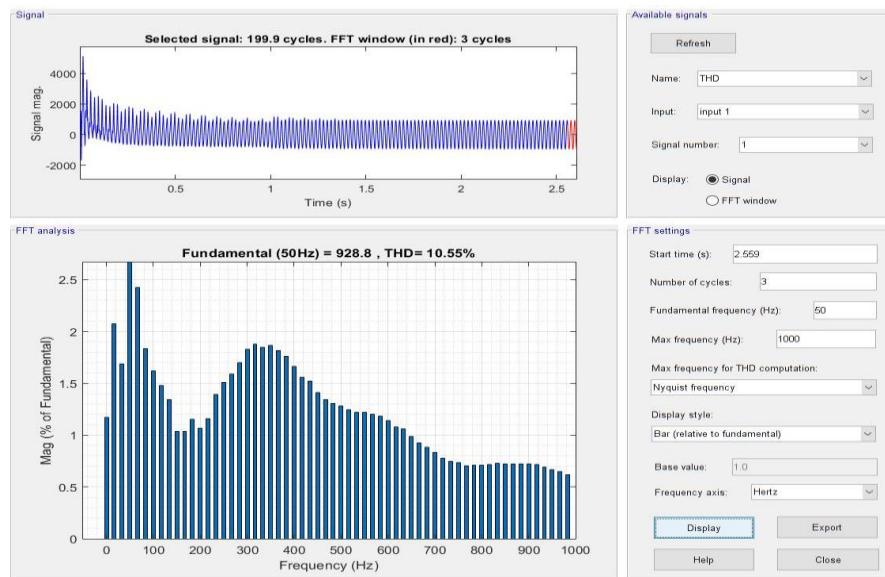
Figure IV.13: Spectrum analysis of the Total Harmonic Distortion for the Current Stator Is

IV.4.4 Discussion and interpretation

It can be seen from figure IV.10 that the tow DPC strategy create a big overshoot at the beginning of the active and reactive powers waveform, at 2.7s we observe that the error increased and the active and reactive powers don't follow their reference. According to Figure IV.11 the DC link voltage follows its reference after an overshoot appears at first seconds. The spectrum analysis in figure IV.12 gives THD=10.55% for current stator Is, which determine the harmonic rate in the case of the use of the DPC. These high harmonics have influence on the active and reactive powers.

IV.5. Conclusion

In this chapter, we covered the modelling and control of a wind turbine based on a double fed induction machine whose rotor is powered by a back-to-back converter. we discussed the control of the back-to-back converter, which allowed us to control through the GSC stage the power factor at the point of connection with the network as well as the voltage across the DC-link. Thus, and in order to verify the system under study, we presented the simulation results using MATLAB/Simulink environment for both rotor side converter and grid side converter. The results of simulation are given to demonstrate the performance of the proposed controllers in the two parts. It can be concluded that the two controllers have succeeded in achieving the desired objectives.

General conclusion

The aim of this work concerns the study, modelling and control of a system of wind energy production. For this, a modelling of the different components of this system was carried out. These models have been used for the development of several techniques of controls to ensure precise and continuous control of the stator powers generated while guaranteeing stability, tracking speed with zero static error. That enabled high system efficiency and optimal production quality.

In the first chapter, we began this work with a reminder about wind energy and the system used to produce this energy, Then, we presented a general description of all the constituent elements of the wind turbine system. Theoretical notions on the horizontal-axis wind turbine are discussed, also covers maximum power point tracking MPPT strategies, which is necessary for maximizing energy extraction. In the second chapter, we carried out a global modelling of the double fed induction generator using in our system in both the abc-coordinate and the dq-coordinate system, which is controlled by the rotor via an inverter and a DC bus placed downstream of this converter, whose connection to the network is carried out by a PWM rectifier which allows bus control DC with power factor regulation on the network side. We applied a direct field-oriented control technique in the machine side converter where we expressed the stator quantities of the DFIG in function of the rotor currents to ensure the control of the machine by the rotor, which was detailed in the third chapter, to independently control the exchange of stator powers produced towards the grid. The control of the grid side converter performs two functions control the currents that flowing in RL filter and control voltage of the DC bus which is detailed in the last chapter. The performances of these last two methods for controlling the stator powers, maintaining the DC bus voltage and unity power factor and a lower total harmonic distortion were justified by the simulation results under MATLAB/Simulink software.

References

[1] Portillo, S. R. (2021, April 12). Qu'est-ce que l'énergie éolienne ? – Fonctionnement et exemples. projetecolo.com. https://www.projetecolo.com/qu-est-ce-que-l-energie-eolienne-fonctionnement-et-exemples-77.html

[2] Wind explained Electricity generation from wind. Energy information administration. https://www.eia.gov/energyexplained/wind/electricity-generation-from-wind.php.

[3] Renewable Energy World. History of wind turbines. https://www.renewableenergyworld.com/storage/gridscale/history-of-wind-turbines/.

[4] Wind turbine parts: An overview. BGB Innovation. https://www.bgbinnovation.com/knowledge/news-and-articles/wind-turbine-partsanoverview.

[5] Tower - Descriptive Information. Energy I-SPARK. https://ei-spark.lbl.gov/generation/onshore-wind/turb/tower/info/

[6] Yektamoghadam, H. Genetic Algorithm and Its Applications in Power Systems Hossein Yektamoghadam, Rouzbeh Haghighi, Majid Dehghani, and Amirhossein Nikoofard. Frontiers in Genetics Algorithm Theory and Applications, 83.

[7] Enel Green Power. (n.d.). Wind turbine. https://www.enelgreenpower.com/learning-hub/renewableenergies/wind-energy/wind-turbine.

[8] Lindy Energy. Wind turbine rotor. https://lindyenergy.com/windturbine-rotor/

[9] Bilbao Carrasco, N. (2024). Application Of Naca Aerodynamic Profile With Tubercle Design On Aerogenerators.

[10] Almihat, M. G. M., & Kahn, M. T. (2022). Wind Turbines Control Trends and Challenges: An Overview. International Journal of Innovative Research and Scientific Studies, 5(4), 378-390.

[11] Lindy Energy. Wind Energy Advantages. https://lindyenergy.com/wind-energy-advantages/

[12] Lindy Energy. Wind Energy Disadvantages. https://lindyenergy.com/wind-energy-disadvantages/

[13] Avaada. Types of Wind Turbines. https://avaada.com/typesof-wind-turbines/

[14] Energy Theory .2 Types of Vertical Axis Wind Turbine. https://energytheory.com/types-of-vertical-axis-wind-turbine

[15] Windmills Tech. Vertical Axis Wind Turbines. https://windmillstech.com/vertical-axis-wind-turbines/

[16] El-Zafry, A. M., El-Hameed, O. E. A., Hassan, M. S., & Shaheen, M. M. (2019). A review on the types of vertical axis wind turbines and the methods of their performance study. J Multidiscipl Eng Sci Technol, 6(9), 10633-10643.

[17] Casonato, A. (2022). A Noiseless Lullaby: Time to Put Wind Wakes to Bed. Fordham Env't L. Rev., 34, 77.

[18] Energydigital. Vortex Bladeless reinvents the wind energy power solution. https://energydigital.com/articles/vortex-bladeless-reinvents-the-wind-energy-power-solution

[19] Wind Energy. The World's Fastest Growing Renewable Energy Resource- An Overview. https://www.ijser.org/paper/Wind-Energy-The-Worlds-Fastest-Growing-Renewable.html

[20] Wikipédia. https://fr.m.wikipedia.org/wiki/_Mat-de-mesure-de-Granges-le-Bourg.

[21] Turbines—Part, W. (2005). 12-1: Power Performance Measurements of Electricity Producing Wind Turbines. British Standard, IEC, 61400-12.

[22] AZZOUZ, Tamaarat. Modélisation et commande d'un système de conversion d'énergie éolienne à base d'une MADA. 2015. Thèse de doctorat. Université Mohamed Khider-Biskra.

[23] Mohammed, A., Ibrahim, J., John, O., & Iliyasu, U. Comparative Study of Horizontal Axis Wind Turbine (HAWT) and Vertical Axis Wind Turbine (VAWT). Department of Electrical and Electronics Engineering, School of Engineering, Hussaini Adamu Federal Polytechnic, Kazaure, Jigawa State, Nigeria.

[24] Jamdade, P. G., Patil, S. V., & Jamdade, S. G. (2013). Assessment of power coefficient of an offline wind turbine generator system. Electronic Journal of Energy & Environment, 1(3).

[25] Cdn. Understanding Coefficient of Power (Cp) and Betz Limit. http://cdn.teachersource.com/downloads/lesson_pdf/betz_limit_0.pdf

[26] Industrie. Les énergies renouvelables principales et les défis qu'elles représentent. https://industrieweb.fr/news/les-energies-renouvelables-principales-et-les-defis-quelles representent.

[27] Wikiwand - Tip-speed ratio. https://www.wikiwand.com/en/Tip-speed_ratio.

[28] Pujari, P. C., Jain, A., Nath, D. S., & Kumar, N. (2021). Performance enhancement of savonius turbine with the application of reorienting blade mechanism. Energy Sources, Part A: Recovery, Utilization, and Environmental Effects, 1-18.

[29] Chavero-Navarrete, E., Trejo-Perea, M., Jáuregui-Correa, J. C., Carrillo-Serrano, R. V., Ronquillo-Lomeli, G., & Ríos-Moreno, J. G. (2020). Hierarchical pitch control for small wind turbines based on fuzzy logic and anticipated wind speed measurement. Applied Sciences, 10(13), 4592.

[30] Govinda, C. V., Udhay, S. V., Rani, C., Wang, Y., & Busawon, K. (2018, March). A review on various MPPT techniques for wind energy conversion system. In 2018 International conference on computation of power, energy, Information and Communication (ICCPEIC) (pp. 310-326). IEEE.

[31] Hamid, C., Derouich, A., Taoussi, M., Zamzoum, O., & Hanafi, A. (2020). An Improved Performance Variable Speed Wind Turbine Driving a Doubly Fed Induction Generator Using Sliding Mode Strategy. 2020 IEEE 2nd International Conference on Electronics, Control, Optimization and Computer Science (ICECOCS).

[32] Eftichios, K. and Kostas, K., Design of a maximum power tracking system for wind energy-conversion applications, IEEE Transaction on industrial electronics, vol. 53, No. 2, pp. 486-494, April 2006.

[33] Tapia, A., Tapia, G., Ostolaza, J.X. and Saenz, J.R. Modeling and control of a wind turbine driven doubly fed induction generator, IEEE Transactions on Energy conversion, vol. 18, No. 2, June 2003.

[34] Wadawa, B., Errami, Y., Obbadi, A., & Sahnoun, S. (2022). Comparison and Choice of MPPT of Wind Turbines Based on Mechanical Wind Generator Speed Control. Prospects of Mechanical Engineering & Technology, 1(1). University Chouaib Doukkali, El jadida, Morocco.

[35] Babu, B., & Divya, S. (2017). Comparative study of different types of generators used in wind turbine and reactive power compensation. IOSR Journal of Electrical and Electronics Engineering, 2, 2320-3331.

[36] Hernández-Mayoral, E., Dueñas-Reyes, E., Iracheta-Cortez, R., Campos-Mercado, E., Torres-García, V., & Uriza-Gosebruch, R. (2021). Modeling and validation of the switching techniques applied to back-to-back power converter connected to a DFIG-based wind turbine for harmonic analysis. Electronics, 10(23), 3046.

[37] DEFONTAINES, Rémi. Etude et Simulation de la MADA. 2012. Thèse de doctorat. École de technologie supérieure.

[38] CHEMIDI, Abdelkarim. Analyse, modélisation et commande avancée d'une éolienne utilisée dans une ferme. 2015. Thèse de doctorat.

[39] VARDHAN, Aanchal Singh S. et SAXENA, Rakesh. Vector control of DFIG-based wind turbine systems. *GMSARN Int J (SCOPUS Indexing), Asian Institute of Technology, Bangkok, Thailand*, 2022, vol. 16, no 04, p. 348-358.

[40] XU, Lie et CARTWRIGHT, Phillip. Direct active and reactive power control of DFIG for wind energy generation. IEEE Transactions on energy conversion, 2006, vol. 21, no 3, p. 750-758.

[41] JENKAL, H., BOSSOUFI, B., BOULEZHAR, A., et al. Vector control of a Doubly Fed Induction Generator wind turbine. Materials Today: Proceedings, 2020, vol. 30, p. 976-980.

[42] SADAOUI, Rabah. Analyse et commande de la machine asynchrone à double alimentation. 2017. Thèse de doctorat. Université du Québec à Trois-Rivières.

[43] Biswas, S. S. (2020). Basics of Vector Control of Asynchronous Induction Motor and Introduction to Fuzzy Controller. Artificial Intelligent Techniques for Electric and Hybrid Electric Vehicles, 241-258.

[44] Rouabhi, R. Contrôle des puissances générées par un système éolien à vitesse variable basé sur une machine asynchrone double alimentée (Doctoral dissertation, Université de Batna 2).

[45] PHAM-DINH, Truc, NGUYEN-THANH, Hai, UCHIDA, Kenko, et al. Modified Controls for Grid-Connected Wind-Turbine Doubly Fed Induction Generator under Unbalanced Voltage Dip for Torque Stability and Reduction of Current Harmonic. In : 2014 Proceedings of the SICE Annual Conference (SICE). IEEE, 2014. p. 1493-1500.

[46] ALLAM, Mohamed, DEHIBA, Boubakeur, ABID, Mohamed, et al. Etude comparative entre la commande vectorielle directe et indirecte de la Machine Asynchrone à Double Alimentation (MADA) dédiée à une application éolienne. Journal of Advanced Research in Science and Technology, 2014, vol. 1, no 2, p. 88-100.

[47] IHEDRANE, Yasmine, EL BEKKALI, Chakib, et BOSSOUFI, Badre. Direct and indirect field oriented control of DFIG-generators for wind turbines variable-speed. In : 2017 14th International Multi-Conference on Systems, Signals & Devices (SSD). IEEE, 2017. p. 27-32.

[48] AMEL FATM, B., & SAMIRA, H. (2020). Etude et analyse de l'effet de déséquilibrage de réseau sur une GADA. Mémoire fin d'étude. Université Ibn-khaldoun de Tiaret.

[49] Fares Eddine, B. (2012). Commande en P et Q de la MADA Alimenté par une Cascade à Trois Niveaux pour La Production de l'Energie Eolienne. Projet De Master. Ecole Nationale Polytechnique.

[50] DEKALI, Z., BAGHLI, L., et LUBIN, A. Boumediene. Grid side inverter control for a grid connected synchronous generator based wind turbine experimental emulator. EJEE 23 (1), 1–7 (2021).

[51] Karaarslan, A., & Ortatepe, Z. (2016). The Grid Side Control of DFIG Based on Wind Turbines.

[52] Song, S.H., Kang, S.I., Hahm, N.K. (2003).Implementation and control of grid connected AC-DCAC power converter for variable speed wind energy conversion system. 18th Annual Applied Power Electronics Conference, Miami Beach, FL, pp. 154-158. https://doi.org/10.1109/APEC.2003.1179207

[53] GAILLARD, Arnaud. Système éolien basé sur une MADA: contribution à l'étude de la qualité de l'énergie électrique et de la continuité de service. 2010. Thèse de doctorat. Université Henri Poincaré-Nancy 1.

[54] EL AZZAOUI, Marouane et MAHMOUDI, Hassane. Modeling and control of a doubly fed induction generator base wind turbine system optimizition of the power. Journal of Theoretical and Applied Information Technology, 2015, vol. 80, no 2, p. 304.